NOVEL METHODS FOR INCREASING EFFICIENCY OF QUANTITATIVE TRAIT LOCUS MAPPING

by

ZHIGANG GUO

M. S., Nanjing Agricultural University, 1998

AN ABSTRACT OF A DISSERTATION

submitted in partial fulfillment of the requirements for the degree of

DOCTOR OF PHILOSOPHY

Department of Plant Pathology
College of Agriculture

KANSAS STATE UNIVERSITY
Manhattan, Kansas

2007

Abstract

The aim of quantitative trait locus (QTL) mapping is to identify association between DNA marker genotype and trait phenotype in experimental populations. Many QTL mapping methods have been developed to improve QTL detecting power and estimation of QTL location and effect. Recently, shrinkage Bayesian and penalized maximum-likelihood estimation approaches have been shown to give increased power and resolution for estimating QTL main or epistatic effect. Here I describe a new method, shrinkage interval mapping, that combines the advantages of these two methods while avoiding the computing load associated with them. Studies based on simulated and real data show that shrinkage interval mapping provides higher resolution for differentiating closely linked QTLs and higher power for identifying QTLs of small effect than conventional interval-mapping methods, with no greater computing time.

A second new method developed in the course of this research toward increasing QTL mapping efficiency is the extension of multi-trait QTL mapping to accommodate incomplete phenotypic data. I describe an EM-based algorithm for exploiting all the phenotypic and genotypic information contained in the data. This method supports conventional hypothesis tests for QTL main effect, pleiotropy, and QTL-by-environment interaction. Simulations confirm improved QTL detection power and precision of QTL location and effect estimation in comparison with casewise deletion or imputation methods.

NOVEL METHODS FOR INCREASING EFFICIENCY OF QUANTITATIVE TRAIT LOCUS MAPPING

by

ZHIGANG GUO

M. S., Nanjing Agricultural University, 1998

A DISSERTATION

submitted in partial fulfillment of the requirements for the degree of

DOCTOR OF PHILOSOPHY

Department of Plant Pathology
College of Agriculture

KANSAS STATE UNIVERSITY
Manhattan, Kansas

2007

Approved by:

Major Professor
James C. Nelson

Abstract

The aim of quantitative trait locus (QTL) mapping is to identify association between DNA marker genotype and trait phenotype in experimental populations. Many QTL mapping methods have been developed to improve QTL detecting power and estimation of QTL location and effect. Recently, shrinkage Bayesian and penalized maximum-likelihood estimation approaches have been shown to give increased power and resolution for estimating QTL main or epistatic effect. Here I describe a new method, shrinkage interval mapping, that combines the advantages of these two methods while avoiding the computing load associated with them. Studies based on simulated and real data show that shrinkage interval mapping provides higher resolution for differentiating closely linked QTLs and higher power for identifying QTLs of small effect than conventional interval-mapping methods, with no greater computing time.

A second new method developed in the course of this research toward increasing QTL mapping efficiency is the extension of multi-trait QTL mapping to accommodate incomplete phenotypic data. I describe an EM-based algorithm for exploiting all the phenotypic and genotypic information contained in the data. This method supports conventional hypothesis tests for QTL main effect, pleiotropy, and QTL-by-environment interaction. Simulations confirm improved QTL detection power and precision of QTL location and effect estimation in comparison with casewise deletion or imputation methods.

Table of Contents

List of Figures

List of Tables

Acknowledgements

First, I thank my advisor Dr. James C. Nelson, for his continuous support and access to academic thinking during my doctoral research. He has been a friend and mentor, and has given me inspiration, encouragement and confidence to solve research problems and write scientific papers. Without his support and guidance, I could not have finished this dissertation.

Secondly, I would like to thank my committee members: Drs. Guihua Bai, Haiyan Wang, Shizhong Xu, and outside chair S. Muthukrishnan, for their friendship, good questions, consideration and encouragement.

Finally, I would like to dedicate this dissertation to my parents Qingen Guo and Cuimei Song, my uncle Qingling Guo and my brother Xiaoqiang Guo. Special thanks go to Xinyan Li, my wife and a caring friend.

CHAPTER 1 - Quantitative trait locus mapping methods: a review

Quantitative traits have been a major area of genetic studies for over a century (Fisher 1918; Wright 1934; Mather 1949; Falconer 1960). In general, observable traits are of two types: quantitative and qualitative. A quantitative trait such as crop yield and human hypertension shows continuous variation, while a qualitative trait such as eye color shows discrete variation. The expression of a trait is called its *phenotype*. The phenotype of a qualitative trait is usually determined by a single gene, while the phenotype of a quantitative trait may be determined by many genes and environmental factors. Early studies of quantitative traits were focused on inferring numbers of genes from the mean, variance, and covariance of progenies, with no knowledge of location of the genes that underlie these traits (Kearsey and Farquhar 1997). Recent development of DNA marker technology allows localizing a gene on a chromosome at the DNA level.

To introduce the genetic background for QTL mapping, I begin by reviewing some basic genetic terminology. In eukaryotes, a *chromosome* is a linear macromolecule composed of DNA. A diploid eukaryotic somatic cell contains multiple pairs of *homologous* chromosomes. *Homology* means similarity by descent from the same ancestral chromosome. For example, corn somatic cells contain 10 pairs of homologous chromosomes. One chromosome of each pair comes from the mother and the other from the father. A parental corn plant produces female or male *gametes* through a process called *meiosis*. Each gamete contains a single copy of each chromosome. During meiosis, two homologous chromosomes first physically pair and exchange segments of homologous DNA, resulting in recombination of genes (discussed below) on each chromosome. The paired chromosomes segregate into different cells to form *gametes*. Male and female gametes fuse to regenerate a plant.

A *gene* is a unit of inheritance. Each gene is a DNA sequence that carries the genetic information determining the expression of a trait. Within a living cell, genes are arranged in linear order along chromosomes. Each chromosome may contain several thousand genes. The position of a gene on a chromosome is called the *locus* of the gene. At each locus, variants of the DNA sequence are called *alleles*. For example, a diploid organism contains two alleles at a locus on two homologous chromosomes. If these two alleles are identical, the organism is said to be *homozygous* at the gene locus. Otherwise, the organism is said to be *heterozygous*. DNA segments used as genetic markers to distinguish different alleles at a given locus are called *DNA markers*. A DNA marker is not necessarily a gene itself, but it provides genetic information to help identify genes close to this marker on the same chromosome.

The genetic constitution of an individual is called its *genotype*. For one gene, the genotype is described by the two alleles at the locus. For example, if there are two alleles *A* and *a* at a locus, there are three possible single-locus genotypes *AA*, *Aa* and *aa* in a population. For multiple genes, the genotype is described by a list of the genotypes at all loci. For example, if there are two genes, and each has two alleles, there are nine possible genotypes in a population: *AABB*, *AABb*, *AAbb*, *AaBB*, *AaBb*, *Aabb*, *aaBB*, *aaBb*, and *aabb*.

Genetic recombination generates allele combinations different from those of either parent. Consider two markers on homologous chromosomes. Marker 1 has two alleles *A* and *a*, while marker 2 has *B* and *b*. Suppose the genotype of P_1 is *AABB* and that of P_2 *aabb*. P_1 and P_2 produce gametes *AB* and *ab* by meiosis. The gametes *AB* and *ab* combine to form a F_1 progeny cell with genotype *AaBb*. By meiosis, a F_1 progeny produces four kinds of gametes: *AB*, *ab*, *Ab* and *aB*. Among these, *AB* and *ab* are parental gametes, and *Ab* and *aB* are *recombinant* gametes carrying alleles from different parents. The ratio of the number of recombinant gametes to the total number of gametes is the *recombination fraction* between the two loci. Loci with recombination fraction below 0.5 are said to be *linked*.

A linear representation of the chromosome with ordered loci is called a *linkage map*. The unit of a linkage map is the centiMorgan (cM), which is genetic distance calculated based on recombination fraction. If there are many loci on the same chromosome, a linkage map (Fig. 1.2) is constructed by arranging these loci on the chromosome according to the recombination fractions between all pairs of loci.

A gene locus on a chromosome determining the phenotype of a quantitative trait is called a *quantitative trait locus* (*QTL*). *QTL mapping* is the process of identifying statistical association between the trait phenotype and marker genotype. For QTL mapping, this association is modeled as

$$y = \mu + \sum_i G_i a_i + e$$

where y is the phenotype, μ the overall mean of the phenotype, G_i the genotype of gene i, a_i the effect of gene i, and e residual error following a normal distribution

$e \sim N(0, \sigma^2)$.

If there are interactions between different genes, *epistasis*, these interactions are easily incorporated as covariates into the model.

The first requirement for QTL mapping is making a mapping population. Suppose *AA* and *aa* are the genotypes of parents 1 (P_1) and 2 (P_2) at each locus. Making a cross between P_1 and P_2 leads to F_1 progeny with genotype *Aa*. Selfing F_1 results in F_2 progeny with the expected genotype proportions *AA* (0.25) : *Aa* (0.50) : *aa* (0.25), and continued selfing of progeny for several generations results in recombinant inbred lines (RILs) with the expected genotype proportions *AA* (0.50) : *aa* (0.50). *Backcrossing* the F_1 to parent P_1 yields BC_1 progeny segregating *AA* (0.50) : *Aa* (0.50). These can be backcrossed in turn to give BC_2 progeny segregating *AA* (0.75) : *Aa* (0.25). F_2, RIL and BC populations are among several types of QTL-mapping population.

Many statistical methods have been developed for QTL mapping. These methods may be classified into least squares, maximum likelihood, and Bayesian estimation. In the following discussion, the main ideas of these methods are introduced in the historical order of their development. Complex statistical details are omitted for simplicity.

Single-marker tests

Single-marker (SM) includes the *t* test, ANOVA (ANalysis Of VAriance) or simple regression. The *t* test and ANOVA focus on testing the difference between phenotypic means of marker genotype classes, while simple regression provides an estimate of marker effect. At a marker, all the progeny is split into distinct groups according to marker genotype and the phenotypic means of the groups are compared. The *t* test can be used in populations such as RIL or BC that have only two genotype classes, while ANOVA is used for populations such as F_2 that have three. A marker showing a significant *t* or *F* test is presumed to be linked to a QTL. Simple regression for SM is based on the linear model

$$y = \mu + ma + e \qquad (1)$$

where y is the phenotype, μ the overall mean of the phenotype, m the genotype of a marker, a the marker effect, and e residual error following a normal distribution

$e \sim N(0, \sigma^2)$.

Based on this model, unknown parameters μ, a, and σ^2 are estimated by the least-squares method, which minimizes the squares of residual errors obtained as the difference between the phenotype and fitted value.

The advantage of SM lies in its simplicity and fast computation. The *t* test, ANOVA, and simple regression are easily implemented in standard software such as SAS, Splus, R or MATLAB. However, this method fails to localize a QTL that lies between two markers.

Interval mapping

Simple interval mapping: Simple interval mapping (SIM) (Lander and Botstein 1989) allows localizing a QTL between two markers. Suppose there is a QTL located between markers 1 and 2. At best, SM returns its highest test statistic for the marker closest to the QTL. With SIM, candidate positions at 1- or 2-cM intervals are tested. At a candidate position, if QTL genotype could be observed, simple regression could be used to identify association between phenotype and genotype based on the genetic model

$$y = \mu + za + e \qquad (2)$$

where z is the genotype of the putative QTL and a is the QTL effect. However, the QTL genotype z is unobservable. But its probability distribution conditional on flanking markers may be inferred, and its expectation of z may then be calculated as

$$E(z) = (+1)p(z = +1 \mid M_{left}, M_{right}) + (-1)p(z = -1 \mid M_{left}, M_{right}).$$

Now a test can be done by the regression of y on $E(z)$ based on model (2). Substitution of unobserved z with its expectation $E(z)$ increases the variance of the fitted phenotype value by the variance caused by uncertainty of the predicted QTL genotype, leading to reduced test statistics especially at testing positions in wide intervals (Xu 1995).

Better estimates of QTL parameters are obtained by an application of the EM algorithm (Lander and Botstein 1989). EM is a variant of maximum likelihood estimation (MLE), performed by iteration of expectation (E) and maximization (M) steps. In the E-step, instead of using only flanking markers to infer conditional probability of QTL genotype (prior probability), this method uses both flanking markers and phenotype to infer posterior probability based on Bayes' Theorem. In the M-step, model parameters μ, a, and σ^2 are estimated by the regression of phenotype on the expectation of QTL genotype calculated based on posterior probability. E and

M steps are repeated until the change in likelihood or parameter estimates is less than a specified value.

The evidence used for the presence of a QTL is LOD (logarithm of odds). It is calculated based on the null hypothesis H_0 of no QTL and alternative hypothesis H_A of a QTL at the tested position as

$$\text{LOD} = -\log_{10}(L_{\text{reduced}} / L_{\text{full}}),$$

where L_{reduced} is the log likelihood of the reduced model, corresponding to H_0, and L_{full} is that of the full model, corresponding to H_A (Lander and Botstein 1989). Repeating this calculation at every point along a chromosome produces a LOD profile on which peaks indicate the presence of QTLs. Fig. 1.3 shows a LOD profile based on a simulated RIL population.

SIM gives more power for QTL mapping than SM due to exploitation of information from a linkage map (Lander and Botstein 1989, Haley and Knott 1992, Zeng 1994). It allows inferring missing genotype of a marker given its flanking markers. However, SIM considers only one QTL at a time for QTL mapping, and does not model multiple QTLs.

Composite interval mapping: Composite interval mapping (CIM) provides a way to model multiple QTLs (Zeng 1993, 1994; Jansen 1993). The genetic model for CIM is

$$y_i = \mu + z_i a + \sum_{j=1}^{c} M_{ij} b_j + e_i \, , \tag{3}$$

where M_{ij} is the genotype of the cofactor marker j of individual i, and b_j the effect of marker j. The basic idea of CIM is that, when testing for a putative QTL at a testing position, one uses other cofactor markers as covariates to remove variation from these QTLs.

QTL parameters are estimated by the ECM (Expectation/Conditional Maximization) algorithm (Zeng 1993, 1994). ECM is a combination of EM and multiple regression in which the E step is the same as that of EM used by SIM, while the CM step involves estimates of cofactor effects by least squares. ECM produces unbiased estimates of QTL and cofactor effects (Zeng 1993, 1994).

Compared with SIM, CIM provides improved power and precision of estimates of QTL location and effect (Zeng 1993, 1994). However, CIM does not determine automatically the number of cofactor markers to be included in the model. If too many are included, they will overestimate the phenotypic variation caused by background QTLs, reducing the significance of tested QTLs. If too few are included, the advantage of CIM over SIM may be insignificant.

Moreover, the amount of QTL variation explained by a cofactor marker decreases with increasing genetic distance between the QTL and the marker.

Multi-trait QTL mapping: Multiple-trait composite interval mapping (multi-trait CIM) provides increased power over single-trait mapping by taking into account the correlated structure of multiple traits (Jiang and Zeng 1995; Korol *et al*1995, 1998). Correlation between different traits is caused by QTLs controlling the expression of those traits, *pleiotropic* QTLs. In multi-trait CIM, these traits are assumed to follow a multivariate normal distribution. The correlation between them is represented by the covariance component in the variance-covariance matrix.

Multi-trait CIM provides formal procedures to test biologically interesting hypotheses concerning the nature of genetic correlation (Jiang and Zeng 1995). These hypothesis tests include QTL main effect, pleiotropy, QTL by environment interaction, and pleiotropy *vs.* close linkage. However, this method fails to accommodate incomplete phenotypic data. Chapter 3 describes an EM-based algorithm for exploiting all the phenotypic and genotypic information contained in the incomplete phenotypic data.

Multiple-interval mapping: Multiple-interval mapping (MIM) uses multiple marker intervals simultaneously to fit multiple QTLs directly in the model for mapping QTL (Kao et al. 1999). With MIM, a stepwise selection procedure with likelihood ratio test statistic as a criterion is used to identify QTL. The procedure begins with no QTL, and then adds or drops QTL one at a time. In the first QTL analysis, one QTL identified using SIM or CIM is incorporated into the model and used as a cofactor for mapping the next QTL. In the QTL analysis, the intervals with a putative QTL and the QTL identified in the first analysis are tested simultaneously in the model. A stepwise regression procedure is used to determine which QTL should be included or dropped from the model for the next QTL search. This process is repeated until the likelihood ratio test for a putative QTL is lower than a critical value. Thus, for a candidate QTL at a testing position, MIM uses QTLs identified in the previous analyses instead of cofactor markers as covariates to adjust genetic background. For this reason it provides better power and precision of QTL mapping than SIM and CIM.

Bayesian QTL mapping

Bayesian QTL mapping provides a flexible way to search for multiple QTLs simultaneously. This method makes inferences about parameters in a way different from MLE or regression-based methods used by SIM or CIM. Based on a probabilistic model with a parameter vector $\mathbf{\Phi} = [\theta_1, \theta_2]$ where $\theta_{1,}\ \theta_1$ are parameters in the model, the likelihood function L is defined as the conditional probability of observations given $\mathbf{\Phi}$. Formally, L can be written as

$$L(\mathbf{\Phi};\mathbf{Y}) = p(\mathbf{Y} \mid \mathbf{\Phi}),$$

where $\mathbf{Y}$ represents a sample from the model. A point estimate of $\mathbf{\Phi}$ can be obtained by maximizing L with respect to θ_1 or θ_2. In the Bayesian approach, inference is based on the posterior probability of $\mathbf{\Phi}$. According to Bayes' Theorem, this is

$$p(\mathbf{\Phi} \mid \mathbf{Y}) = \frac{p(\mathbf{\Phi},\mathbf{Y})}{p(\mathbf{Y})} = \frac{p(\mathbf{\Phi},\mathbf{Y})}{\sum_{\Phi} p(\mathbf{\Phi},\mathbf{Y})} = \frac{p(\mathbf{\Phi})p(\mathbf{Y} \mid \mathbf{\Phi}\,|)}{\sum_{\Phi} p(\mathbf{\Phi})p(\mathbf{Y} \mid \mathbf{\Phi}\,|)}, \tag{4}$$

where $p(\mathbf{\Phi})$, the prior probability of $\mathbf{\Phi}$, quantifies the knowledge we have about θ_1 and θ_2 prior to analysis. In general, it is difficult to calculate joint posterior probability $p(\theta_1, \theta_2\ |\mathbf{Y})$ in closed form from equation (4), but easy to calculate the marginal posterior probability of θ_1 or θ_2 as

$$p(\theta_1 \mid \mathbf{Y},\theta_2) = \frac{p(\mathbf{Y} \mid \theta_1,\theta_2)p(\theta_1)}{\sum_{\theta_1} p(\mathbf{Y} \mid \theta_1,\theta_2)p(\theta_1)} \tag{5}$$

given fixed θ_2, and

$$p(\theta_2 \mid \mathbf{Y},\theta_1) = \frac{p(\mathbf{Y} \mid \theta_1,\theta_2)p(\theta_2)}{\sum_{\theta_2} p(\mathbf{Y} \mid \theta_1,\theta_2)p(\theta_2)} \tag{6}$$

given fixed θ_1. Sampling $\mathbf{\Phi}$ from $p(\mathbf{\Phi}|\ \mathbf{Y})$ is replaced with drawing θ_1 and θ_1 in turn from their marginal posterior probability distributions [equations (5) and (6)]. This strategy is called Gibbs sampling. Continued sampling of this kind is known as the Markov-chain Monte Carlo (MCMC) method, because the previous sample values are used as parameters to sample the next values, generating a Markov chain. Fig. 1.5 gives an example of Bayesian QTL mapping based on simulation.

With Bayesian QTL mapping methods, the most difficult problem is sampling the posterior probability of QTL number. While QTL location and effect are relatively easy to sample, determining QTL number is a problem of model selection (Broman and Speed 2002).

Models with different number of QTLs are compared, and the best one is selected based on a specific selection criterion such as AIC or BIC. In Bayesian analysis, the optimal model is selected by a probabilistic jump of MCMC from a model with m QTLs to a new one with $m + 1$ or $m - 1$ QTLs. Reversible-jump MCMC (RJMCMC) (Green 1995) provides a method for realizing this jump between models with different number of QTLs. RJMCMC has been applied in many Bayesian QTL mapping methods for identifying multiple QTLs (Thomas et al. 1997; Sillanpää and Arjas 1998; Stephens and Fisch 1998; Yi and Xu 2000; Gaffney 2001; Yi and Xu 2002; Yi et al. 2003; Narita and Sasaki 2004). However, it requires much more computation than SIM or CIM, and its convergence is very sensitive to the specification of prior probabilities of parameters.

A recent development in Bayesian QTL mapping, the shrinkage Bayesian method, includes all markers in a model simultaneously in a single test (Xu 2003). When the number of markers is larger than that of individuals, the model is oversaturated. The problem of the oversaturated model is that it cannot provide unique estimates of marker effects. With the shrinkage Bayesian method, the problem is solved by the assumption that the effect of each marker follows a normal distribution with its own mean and variance. The assumption is used to limit large fluctuation of marker effect estimates, and obtain unique estimates. This leads to shrinkage estimates of marker effects, resulting in clear signals of QTL effects. Based on shrinkage estimation, spurious QTL effects are shrunk towards zero, while real QTL effects are estimated with virtually no shrinkage. Penalized MLE (PMLE) (Zhang *et al.* 2005), an extension of the shrinkage method in MLE, was developed to reduce the computation associated with the shrinkage method and analyze marker-marker interaction. However, PMLE and shrinkage Bayesian mapping are marker-based mapping methods. They cannot be used for interval mapping.

Shrinkage interval mapping (shrinkIM) method (see more details in chapter 2) extends PMLE and shrinkage Bayesian method to interval mapping. It combines the advantages of shrinkage Bayesian method and PMLE. This method allows analyzing QTL and QTL epistasis based on mapping populations.

References

Broman K. W., and Speed T. P., 2002 A model selection approach for the identification of quantitative trait loci in experimental crosses. Journal of the Royal Statistical Society **64**: 641-656

Calinski T., Kaczmarek Z., Krajewski P., Frova C. and Sari-Gorla M., 1999 A multivariate approach to the problem of QTL localization. Heredity **84**: 303-310.

Doerge R. W., 2001 Mapping and analysis of quantitative trait loci in experimental populations. Nature Genetics **3**:43-52

Falconer D. S. 1960 Introduction to Quantitative Genetics, Oliver and Boyd, Edinburgh.

Fisher R. A. 1918 The correlation between relatives on the supposition of Mendelian inheritance. Philosophical Transactions of the Royal Society of Edinburgh 52: 399-433.

Green P. J., 1995 Reversible jump Markov chain Monte Carlo computation and Bayesian model determination. Biometrika **57**: 97–109.

Haley C. S. and Knott S.A., 1992 A simple regression method for mapping quantitative trait loci in line crosses using flanking markers. Heredity **69**: 315-324.

Jansen R. C. 1994 Genotype-by-environment interaction in genetic mapping of multiple quantitative trait loci. Theoretical and Applied Genetics **91**: 33-37.

Jiang C. J., and Zeng Z. B., 1995 Multiple trait analysis of genetic mapping for quantitative trait loci. Genetics **140**: 1111-1127.

Kearsey M. J., Farquhar G. L. F., 1997 QTL analysis in plants; where are we now?. Heredity **80**: 137-142

Korol A. B., Ronin Y. I. and Kirzhner V. M.. 1995 Interval mapping of quantitative trait loci employing correlated trait complexes. Genetics **140**: 1137-1147.

Korol A. B., Ronin Y. I., Nevo E. and Hayes P. M.. 1998 Multi-interval mapping of correlated trait complexes. Heredity **80**: 273-284.

Mather K. 1949 Biometrical Genetics, 1st edition. Methuen, London.

Lander E. S., and Botstein D., 1989 Mapping Mendelian factors underlying quantitative traits using RFLP linkage maps. Genetics **121**:185-199.

Sillanpää M. J. and Arjas E., 1998 Bayesian mapping of multiple quantitative trait loci from incomplete inbred line cross data. Genetics **148**: 1373-1388.

Sillanpää M. J. and Arjas E., 1999 Bayesian mapping of multiple quantitative trait loci from incomplete outbred offspring data. Genetics **151**: 1605-1619.

Wright S. 1934 An analysis of variability in number of digits in an inbred strain of guinea pigs. Genetics 19:506-536.

Xu S., 1995 A comment on the simple regression method for interval mapping. Genetics **141**: 1657-1659.

Xu S., 2003 Estimating polygenic effects using markers of the entire genome. Genetics **163**: 789-801.

Zeng Z. B., 1993 Theoretical basis of precision mapping of quantitative trait loci. Proceedings of the National Academy of Sciences USA **90**: 10972-10976.

Zeng Z. B., 1994 Precision mapping of quantitative trait loci. Genetics **136**: 1457-1468.

Figure 1.1 Histograms of qualitative and quantitative traits.

Figures *a* and *b* show the phenotypic frequency distributions of a qualitative and a quantitative trait in a sample with 100 individuals. In *b*, the phenotype of a trait was simulated from a normal distribution with mean 40 or 100 and standard deviation 20.

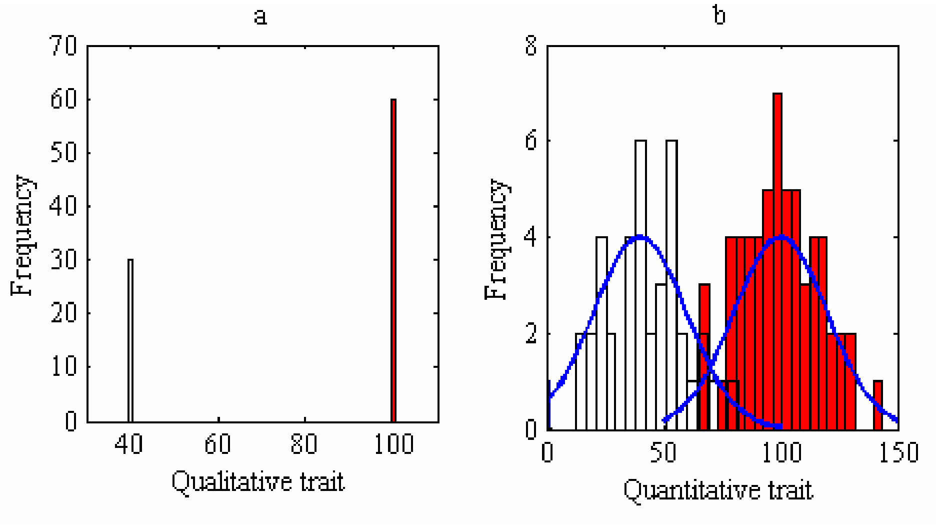

Figure 1.2 A rice linkage map.

The genotypic data used was from a rice QTL study focused on improving grain yield of U.S. rice varieties (http://www.uark.edu/ua/ricecap)

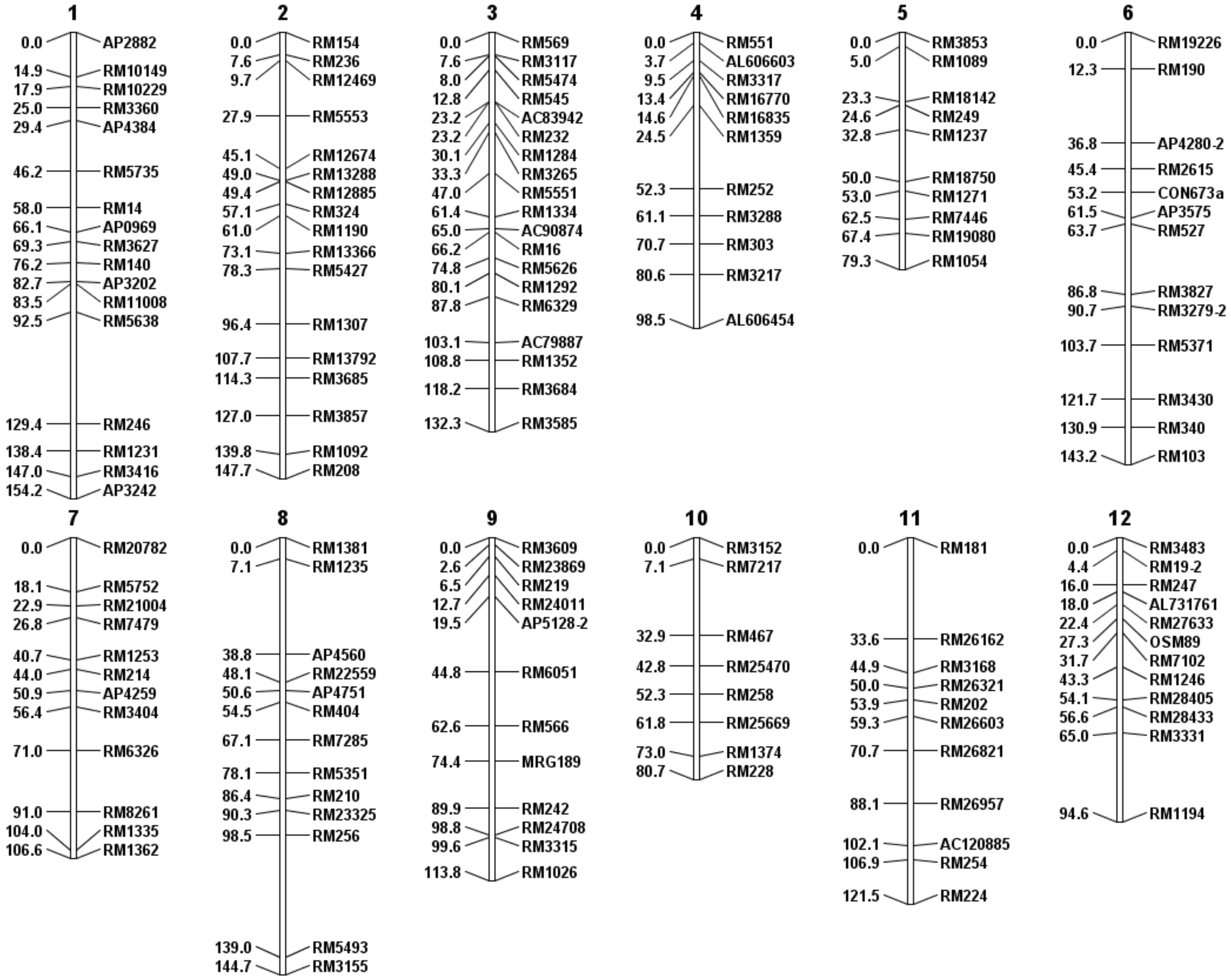

Figure 1.3 LOD profiles produced by SM, SIM and CIM methods for QTL mapping. SM: single-marker mapping; EM-based SIM: EM-based simple interval mapping; regression-based SIM: regression-based simple interval mapping; CIM: composite interval mapping. The horizontal black dashed line represents 0.05 significance level LOD threshold 2.17 estimated from 1000 permutation tests with regression-based SIM. The blue dots on the SM curve show effect and location of each marker.

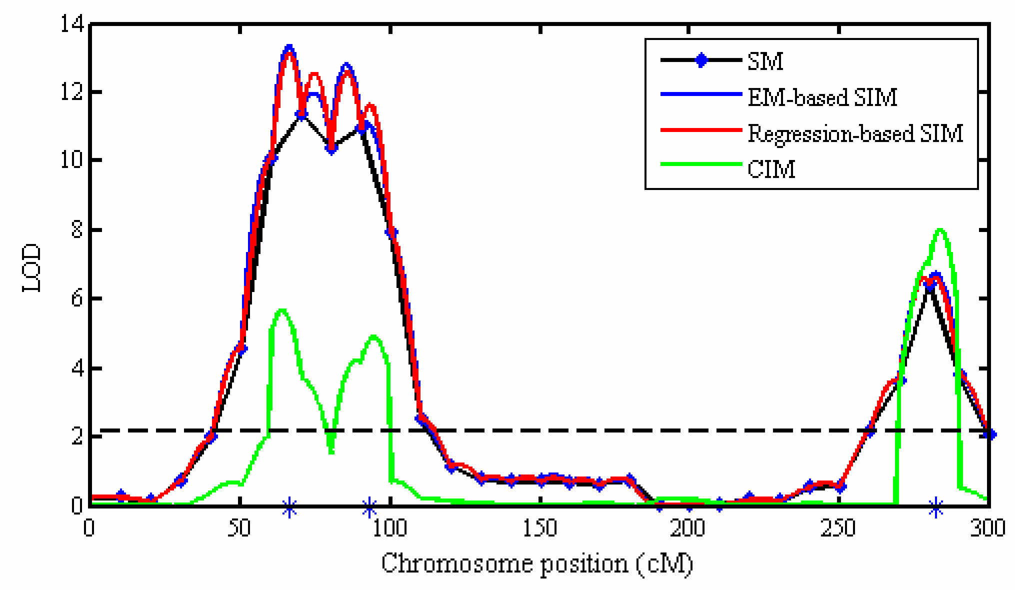

Figure 1.4 Posterior distributions of QTL parameters from Bayesian QTL mapping with simulated data

Posterior frequencies of QTL number and locations were calculated from 2000 MCMC iterations based on a simulated RIL population with 300 individuals. Fig. *a*: a plot of QTL number over iterations. Fig. *b*: Posterior frequency of QTL number. Fig. *c*: posterior frequency of QTL location on chromosome 1. Fig. *d*: posterior frequency of QTL location on chromosome 2. Asterisks show the true positions of simulated QTLs.

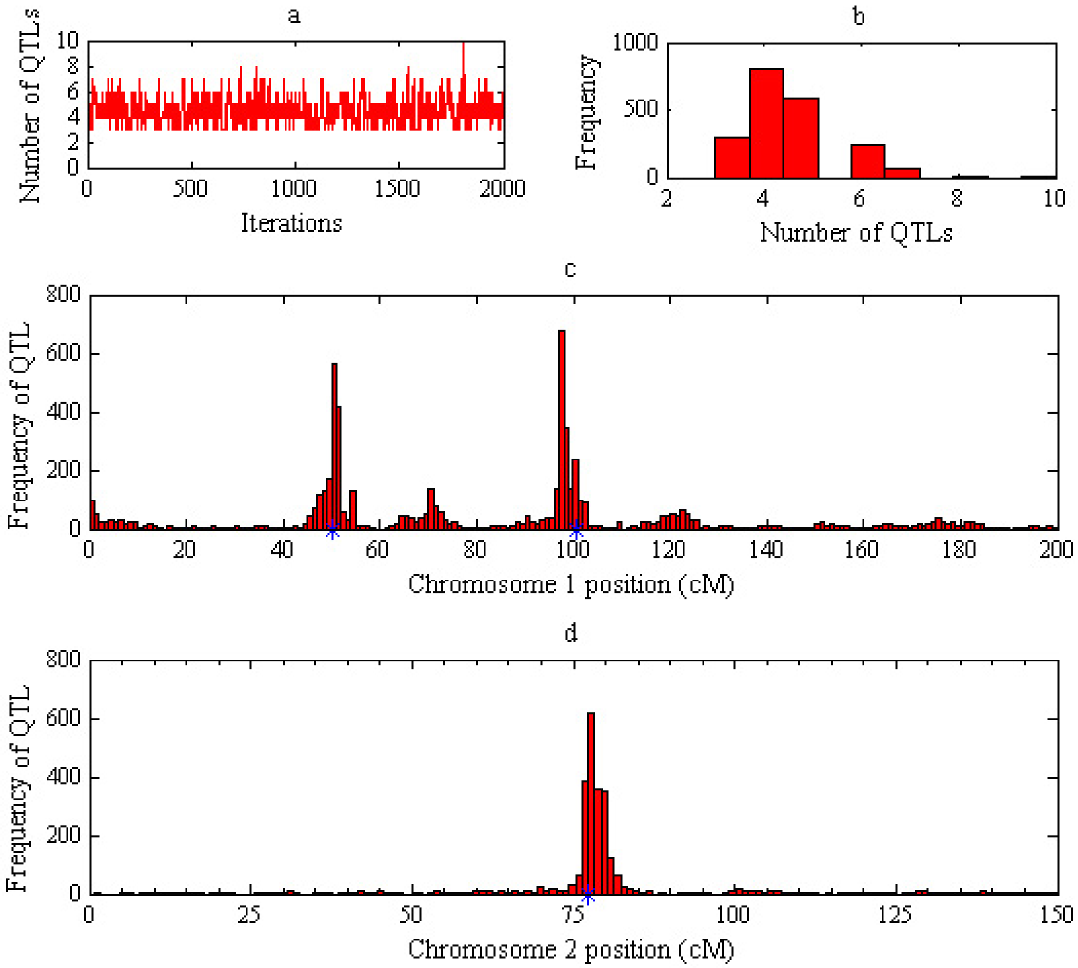

CHAPTER 2 - Shrinkage interval mapping for QTL and QTL epistasis analysis in line crosses

Abstract

QTL modeling is an example of an oversaturation problem, requiring the choice of a subset from an excess of explanatory variables. Shrinkage Bayesian and penalized maximum likelihood estimation (PMLE) approaches have been shown to give increased power and resolution for estimating QTL main or epistatic parameters. However, Bayesian methods are computationally expensive and PMLE cannot localize a QTL within an interval. We describe a two-step shrinkage interval-mapping method, shrinkIM, which addresses both weaknesses. In the first step, PMLE is used to select cofactor markers or pairwise marker–marker interactions, reducing the dimensionality of the oversaturated model. In the second step, partially penalized maximum likelihood estimation (PPMLE) is used for QTL interval mapping or QTL epistasis analysis. PPMLE, in which only the parameter of interest — QTL main or epistatic effect — is penalized, provides shrinkage estimates of these effects as well as least-squares estimates of other parameters in the model. Studies based on simulated and real data show that shrinkIM provides higher resolution for differentiating closely linked QTLs and higher power for identifying QTLs of small effect than conventional interval mapping methods, with no greater computing time.

Introduction

Interval-mapping methods for finding a predictive relationship between DNA marker genotypes and quantitative-trait phenotypes fall into three general statistical classes: likelihood maximization by EM algorithm used for simultaneous estimation of genotype and trait distribution parameters (Lander and Botstein 1989); least-squares estimation by regression of phenotypes on QTL genotype expectations (Haley and Knott 1992); and Bayesian methods. The last approach treats all parameters as random variables and constructs their posterior distributions given priors, using Markov chain Monte Carlo estimation (Satagopan *et al.* 1996; Sillanpää and

Arjas 1997, 1999; Yi and Xu 2001; Wang *et al.* 2005). Various extensions of the first two approaches have been developed for modeling multiple QTL (Zeng 1994), QTL–environment interaction (Jansen 1994), multiple traits (Jiang and Zeng 1995; Hackett *et al.* 2001; Korol *et al.* 2001) and multiple interval mapping (Kao *et al.* 1999). All approaches face the difficult model-selection problem: finding a reduced model to explain the response (phenotype data) in the presence of numbers of explanatory variables (DNA markers) that exceed the number of observational units (individuals) such that there is no unique solution to a full model.

Recent approaches to this problem, while incorporating all the markers, apply shrinkage (Groß, 2003, p. 150) to reduce the effective dimension of the model. Shrinkage methods penalize model coefficients by treating them as drawn from a normal distribution centered on zero, thereby "shrinking" them toward a prior mean of zero (Boer *et al.* 2002). Two shrinkage approaches have been suggested: Bayesian and penalized likelihood, the latter including penalized regression such as ridge regression. Typical of shrinkage methods is a QTL profile scan showing a near-zero baseline over most of the genome map, with a few QTL signals standing out conspicuously.

Bayesian shrinkage method: Xu (2003) developed a Bayesian regression method, multiple-marker analysis, for simultaneously estimating the genetic effect associated with the markers along the whole genome map. Each marker effect is allowed to have its own variance parameters so that the variance can be estimated from the data. Wang *et al.* (2005) extended this method to allow localizing a QTL within an interval, using Metropolis-Hastings sampling since the QTL location parameter does not have an explicit posterior distribution. However, the Bayesian method is time-consuming to compute.

Ridge regression: Consider the linear model $\mathbf{Y} = \mathbf{X}\boldsymbol{\beta} + \boldsymbol{\varepsilon}$, where $\mathbf{Y}$ is a $n \times 1$ trait vector, $\mathbf{X}$ a $n \times m$ marker matrix, $\boldsymbol{\beta}$ a $m \times 1$ vector of regression coefficients, and $\boldsymbol{\varepsilon}$ a $n \times 1$ random error vector with $\varepsilon \sim \mathrm{N}(0, \mathbf{I}_n\sigma^2)$. For an oversaturated model, ordinary least-squares estimates of $\boldsymbol{\beta}$ cannot be calculated as $(\mathbf{X'X})^{-1}\mathbf{X'Y}$ because matrix $\mathbf{X'X}$ is singular. However, ridge regression can provide a restricted least-squares estimate as $(\mathbf{X'X} + \tau\,\mathbf{I}_n)^{-1}\mathbf{X'Y}$ under the quadratic constraint $\Sigma\beta_j^2 < \tau$ (τ: a penalty parameter) on $\boldsymbol{\beta}$. Boer *et al.* (2002) proposed the use of ridge regression for QTL epistasis analysis, allowing the penalties to vary with regression coefficient. However, inversion of matrix $\mathbf{X'X} + \tau$ In becomes time-consuming with increasing numbers of regression coefficients $\boldsymbol{\beta}$.

Penalized maximum-likelihood estimation: The penalized maximum-likelihood estimation (PMLE) method suggested by Zhang and Xu (2005) imposes a prior normal distribution N(μ_j , σ_j^2) penalty on each β_j, allowing the penalty to vary across $\boldsymbol{\beta}$. An iterative algorithm is used to estimate regression coefficients $\boldsymbol{\beta}$ and other parameters. In essence, PMLE is an extension of the multiple-marker Bayesian method of Xu (2003). However, PMLE can localize a QTL only to a marker and not between markers.

Shrinkage interval mapping: The foregoing efforts demonstrated that shrinkage estimation methods can provide increased resolution and power as well as low background, but have a few disadvantages. To deal with these we have developed shrinkage interval mapping (shrinkIM), a two-step method. In the first, dimension-reducing step, cofactor markers or marker–marker interactions are selected as suggested by Zhang and Xu (2005) using PMLE, turning the oversaturated model into a regular model. In the second step, a partially penalized maximum likelihood estimation (PPMLE) method — a hybrid of PMLE and least squares — is used to estimate parameters. Instead of penalizing all βs in a model as does PMLE, PPMLE imposes a prior normal-distribution penalty only on the parameter of interest (QTL main or epistatic effect) so that a shrinkage estimate can be obtained. Estimates of other βs are calculated by least squares. In the following description, since PMLE, the method used for cofactor selection, is identical with Zhang and Xu's method (2005), we will focus on PPMLE as used in the second step of shrinkIM.

Methods

One-QTL model for shrinkIM: The method described here is based on a RIL (recombinant inbred line) design but is easily extended to backcross, F_2, or other designs. The linear model for shrinkIM is

$$y_i = \mu + z_i\alpha + \sum_{j=1}^{p} x_{ij}c_j + \varepsilon_i \qquad (1)$$

Here y_i is the trait value of individual i; μ is the overall mean; z_i is the genotype of a QTL for individual i; α is the additive effect of the QTL; x_{ij} is the genotype of the jth cofactor marker in the ith individual and is a dummy variable taking the values 1, 0, and -1 for genotypes A_1A_1, A_1A_2 (rare in RILs) and A_2A_2; c_j is the effect of the jth cofactor marker; ε_i is the residual error of the ith individual with a N(0, σ^2) distribution; and p is the total number of cofactor markers. QTL genotype z_i is not observed and is replaced in the model with its expectation, calculated from the probability distribution of QTL genotype conditional on the closest flanking markers (Haley and Knott 1992). Missing x_{ij} genotype data is similarly imputed.

In this model, the parameter in which we are interested is QTL effect α, while other regression coefficients including overall mean and effects of cofactor markers are treated as nuisance parameters, included only to account for background (polygenic variation). We may combine these and rewrite model (1) in matrix form as

$$\mathbf{Y} = \mathbf{Z}\alpha + \mathbf{X}\boldsymbol{\beta} + \boldsymbol{\varepsilon} \tag{2}$$

where n is the number of individuals, $\mathbf{Y}$ a $n \times 1$ vector of trait values, $\mathbf{Z}$ a $n \times 1$ vector of QTL genotype expectations, α the additive effect of the QTL, $\mathbf{X}$ a $n \times (p + 1)$ matrix with the first column composed of n ones, $\boldsymbol{\beta}$ a vector of regression coefficients $(\mu, c_1, c_2, \ldots, c_p)'$, and $\boldsymbol{\varepsilon} \sim N(0, \mathbf{I}_n\sigma^2)$.

To estimate parameters α, $\boldsymbol{\beta}$ and σ^2, we introduce partially penalized maximum likelihood estimation (PPMLE), a hybrid of penalized maximum likelihood and least squares estimations. Our aim is to obtain shrinkage estimates of parameters of interest in order to realize the advantages associated with shrinkage Bayesian or PMLE, including increased QTL resolution, high power and low background. First we apply to α the penalty function $N(\mu_\alpha, \sigma_\alpha^2)$ from PMLE, imposing a normal distribution in order to limit the fluctuation of α. Then we specify the direction of shrinkage of α by placing the second penalty $N(0, \sigma_\alpha^2 / \eta)$ on the mean μ_α of α, where $\eta > 0$ denotes a prior sample size (Zhang and Xu 2005). In this way we force α to shrink towards zero. The log likelihood functions for model (1) before and after penalization are

$$\log(L) = 0.5n\log(2\pi\sigma^2) - \frac{1}{2\sigma^2}(\sum_{i=1}^{n}(y_i - (\mu + z_i a + \sum_j x_{ij}c_j))^2 \tag{3}$$

and

$$\begin{aligned}\log(L_{penalized}) = {} & -0.5n\log(2\pi\sigma^2) - \frac{1}{2\sigma^2}\sum_{i=1}^{n}(y_i - (\mu + z_i a + \sum_j x_{ij}c_j))^2 \\ & - 0.5\log(2\pi\sigma_\alpha^2) - \frac{1}{2\sigma_\alpha^2}(a - \mu_\alpha)^2 - 0.5\log(2\pi\frac{\sigma_\alpha^2}{\eta}) - \frac{\eta}{2\sigma_\alpha^2}\mu_\alpha^2\end{aligned} \ . \tag{4}$$

In practice, an iterative two-step algorithm may be used to estimate the parameters. It starts with initial values for $\boldsymbol{\theta}^{(0)} = (\alpha^{(0)}, \boldsymbol{\beta}^{(0)}, \sigma^{2(0)}, \mu_\alpha^{(0)}, \sigma_\alpha^{2(0)})$, setting iteration counter $k = 0$. In step 1, we calculate the least-squares estimate of $\boldsymbol{\beta}$ given α,

$$\boldsymbol{\beta}^{(k+1)} = (\mathbf{X'X})^{-1}\mathbf{X'}(\mathbf{Y} - \mathbf{Z}a^{(k)}) \,.$$

In step 2, estimates of α and hyperparameters μ_α and σ_α^2 are calculated by maximizing penalized log likelihood function (4) given $\boldsymbol{\beta}$ as

$$a^{(k+1)} = \frac{\mathbf{Z'}(\mathbf{Y} - \mathbf{X}\boldsymbol{\beta}^{(k)}) + \dfrac{\mu_\alpha \sigma^{2(k)}}{\sigma_\alpha^{2(k)}}}{\mathbf{Z'Z} + \dfrac{\sigma^{2(k)}}{\sigma_\alpha^{2(k)}}},$$

$$\sigma^{2(k+1)} = \frac{1}{n}(\mathbf{Y} - \mathbf{Z}a^{(k)} - \mathbf{X}\boldsymbol{\beta}^{(k)})'(\mathbf{Y} - \mathbf{Z}a^{(k)} - \mathbf{X}\boldsymbol{\beta}^{(k)}),$$

$$\mu_\alpha^{(k+1)} = \frac{\alpha^{(k)}}{\eta + 1},$$

$$\sigma_\alpha^{2(k+1)} = 0.5[(\alpha^{(k)} - \mu_\alpha^{(k)})^2 + \eta\mu_\alpha^{2(k)}].$$

Steps 1 and 2 are repeated until norm $||\boldsymbol{\theta}^{(k)} - \boldsymbol{\theta}^{(k-1)}|| < \tau$, where τ is a given critical value; we used 0.00001.

A likelihood ratio test under the null hypothesis H_0: $\alpha = 0$ and the alternative hypothesis H_A: $\alpha \neq 0$ is LRT = –2 ln ($L_{\text{reduced}} / L_{\text{full}}$), where L_{reduced} is the log likelihood of the reduced model, corresponding to the null hypothesis, and L_{full} is that of the full model, corresponding to the alternative hypothesis (Lander and Botstein 1989). Both are calculated from equation (3) and a LOD score is calculated as LRT/(2 ln 10).

QTL epistasis model for shrinkIM: The linear model for pairwise QTL interaction is

$$y_i = \mu + z_{ir}\alpha_r + z_{is}\alpha_s + z_{ir}z_{is}\alpha_{rs} + \sum_{j=1}^{p} x_{ij}c_j + \sum_{u \neq v}^{q} x_{iu}x_{iv}w_{uv} + \varepsilon_i \tag{4}$$

where α_{rs} is the interaction effect between QTL r and s ($r \neq s$) and w_{uv} the interaction effect between markers u and v ($u \neq v$). Now the parameters of interest are α_r, α_s and α_{rs}, and the other regression coefficients are treated as nuisance parameters. Model (4) can be rewritten as model (2) and parameters estimated using PPMLE. The hypothesis test for QTL epistasis is H_0: $\alpha_{rs} = 0$ and the alternative hypothesis H_A: $\alpha_{rs} \neq 0$. The LOD may be obtained as in the one-QTL model.

It will be noted that pairwise interactions may be detected even between QTLs neither of which exerts a main effect.

Simulation studies: The properties of the shrinkIM algorithm were compared with those of conventional interval-mapping methods, based on simulated and real data. The prior value η = 5 was used in the analysis of simulation or real data, but in tests, no difference was found with values of 10 or 20, echoing the finding of Zhang and Xu (2005). The initial values of prior parameters μ_α and σ_α^2 were set to 0 and 0.1. Power to detect a given QTL was calculated as the proportion of replicates showing a LOD peak above threshold within the interval containing the QTL (Haley and Knott 1992; Jiang and Zeng 1995; Zhang and Xu 2005). All calculations were implemented in MATLAB (The MathWorks, Inc.), a mathematical and statistical computing language.

In each of two simulation experiments, RIL populations of 300 individuals were generated based on a 300-cM chromosome with 31 evenly spaced markers. The model for the simulation is

$$y_i = \sum_{j=1}^{n_{QTL}} \alpha_j q_{ij} + \sum_{k=1}^{n_{EPI}} \alpha_{mn} q_{im} q_{in}$$

where y_i is the phenotype of individual i, α_j is the main effect of QTL, α_{mn} is the epistatic effect of QTL m and n, n_{QTL} is the number of main effects, n_{EPI} is the number of epistatic effects, q_{ij} is the genotype of QTL j of individual i. Environmental error for y_i was sampled from a normal distribution with mean zero and variance σ^2. In both experiments, the calculation interval (step size) used for interval mapping was 1 cM. Cofactors for CIM were selected by forward stepwise regression; those for PMLE by the criterion $|b_j|/\sigma > 10^{-6}$, where b_j is the estimate of effect of marker j and σ is the estimate of the error standard deviation.

Experiment I: The resolution and background level for the detection of QTL or QTL epistasis in a single simulated population were examined. A RIL population was simulated according to the QTL parameters given in Table 2.1. Two types of analyses were performed to identify QTL main and epistatic effects respectively.

Analysis 1: A one-QTL model was used to detect QTL main effect using shrinkIM and marker-based analyses including single-marker analysis (regression of phenotype on genotypes of individual markers), multiple-marker analysis using PMLE (Zhang and Xu 2005) and the Bayesian approach (Xu 2003). ShrinkIM was compared with simple interval mapping by regression (SIM) (Haley and Knott 1992), and CIM (Zeng 1994). The EM-based version EM-SIM (Lander and Botstein 1989) was also computed, but since the results were virtually identical to those of SIM, we used this method only for speed comparison. The evidence for the identification of a QTL was evaluated based on QTL effect and LOD score. The same three cofactor markers were used in both shrinkIM and CIM. We also calculated a variant of the main-effect model that included four marker–marker interaction cofactors calculated by PMLE. In order to test the sensitivity of the estimate of QTL effect to the choice of prior parameters μ_α and σ_α^2, we ran a separate set of shrinkIM analyses in which the initial μ_α and σ_α^2 were varied independently along the respective ranges [–5:5] and [0.1:1] and the means and standard deviations of QTL effect estimates at each point on the map were computed.

Analysis 2: The QTL-epistasis model was used. ShrinkIM was first compared with PMLE and then with a two-dimensional scan by SIM. In the comparison of shrinkIM and PMLE, only QTL epistatic effect was used as evidence to claim QTL interaction, since a LOD test statistic is not available for PMLE.

Experiment II*:* We simulated 500 replicates of 300 individuals according to the QTL positions and effects given in Table 2.3. The statistical power, accuracy, and precision of QTL detection using the same three interval-mapping methods were compared at three significance levels: $\alpha = 0.05$, 0.01 or 0.001. The LOD threshold for each method was calculated from an additional 2000 simulations with the same total variance of 52.17 but no QTLs.

Analysis of rice data: The phenotypic and genotypic data used for QTL mapping came from a QTL study in rice (http://www.uark.edu/ua/ricecap). A population of 129 RILs from the cross of U.S. rice lines RT0034 x Cypress genotyped at 155 SSR marker loci along a 1500-cM map of 12 chromosomes was used for the detection of QTL affecting days to heading. The mean length of marker intervals was 10.6 cM, with the longest interval 40.5 cM. The population was phenotyped at three locations in Arkansas, Texas and Louisiana with two replicates for each location. Two QTL have been identified from the data of Texas and Louisiana using CIM (results not shown). This prior knowledge was used as a reference for the analysis of Arkansas data. For simplicity, we analyzed only one replicate from Arkansas to illustrate the difference between results from SIM, CIM and shrinkIM. As with the simulated data, we used the same set of cofactor markers for both shrinkIM and CIM.

Results

Simulation experiment I: Fig. 2.1 shows the more accurate estimation of QTL positions and effects using shrinkIM compared to single-marker or multiple-marker analysis. The background signal from PMLE or Bayesian based multiple-marker analysis is the same as that of shrinkIM.

Fig. 2.2 shows the increased resolution of shrinkIM of closely linked QTLs 1 and 2 based on QTL effect and on LOD score compared with SIM or CIM. ShrinkIM gave sharper separation than CIM of closely linked QTLs 1 and 2 based on either effect (Fig. 2.2a) or LOD score (Fig. 2.2b) and reduced the background effect to baseline, while SIM was unable to separate the linked QTLs and consistently overestimated QTL and background effects (Figs. 2.2a). For this simulated dataset, the inclusion of marker–marker interactions as cofactors made no appreciable difference to the results.

Table 2.2 shows comparison of computing times used for 1000 permutations in SIM, EM-SIM, CIM, and shrinkIM in analysis 1, showing that shrinkIM is faster than CIM and EM-SIM. We attribute this to the fewer iterations required in the PPMLE step.

QTL effect estimates proved to be very insensitive to variation in initial values for hyperparameters μ_α and σ_α^2. Their standard deviation across at least ten values was less than 10^{-5}, negligible in comparison with the estimated effect size of ~3.

Fig. 2.3 shows 3D plots of QTL epistatic effect against chromosome positions; not visible is a spurious close double peak produced by the PMLE method. As with main QTL effects, shrinkIM is expected to provide more accurate estimates of positions of QTL interactions than PMLE, since the latter is limited to testing marker positions, while shrinkIM can localize QTL at any position on the genetic map. Table 2.1 compares position and effect estimates from shrinkIM with those of PMLE for the detection of QTL main and epistatic effect. The background signal of shrinkIM is comparable to that of PMLE (Fig. 2.3a). 2D SIM was not able to identify QTL-QTL interaction based on only QTL epistatic effect due to strong background, whereas shrinkIM clearly identified three QTL epistatic effects.

Fig. 2.4 shows the 3D LOD surface of QTL epistasis using 2D SIM and shrinkIM. 2D SIM finds two QTL interactions, while shrinkIM finds three (Fig. 2.4b). Moreover, the LOD surface produced by shrinkIM is much clearer than that of 2D SIM due to decreased background (Fig. 2.4a).

Experiment II: For the detection of QTL 1 and 2 with higher heritability compared to QTL 3, the power of SIM, CIM and shrinkIM was similar. Fig. 2.5 shows the increased power of shrinkIM for the detection of QTL 3 with relatively lower heritability compared with SIM or CIM. The accuracy and precision of estimates of QTL effects and positions are very close for CIM and shrinkIM (Table 2.4).

Analysis of rice data: Fig. 2.6 shows the increased power of shrinkIM for the detection of the QTL on chromosome 6 based on QTL effect or LOD score. In SIM and CIM analysis, the QTL on chromosome 8 was identified, but neither method found the second one, a QTL expressed strongly in the other growing locations and possibly representing *Hd6a*, a QTL identified near the rice *Waxy* locus in several other crosses. Position and effect estimates for the two QTL are given in Table 2.5.

Discussion

We have shown the advantages of shrinkIM over conventional SIM and CIM in the detection and identification of QTL or QTL epistasis. ShrinkIM offered higher resolution of closely linked QTL, greater power to identify QTL and more accurate estimates of QTL parameters without increased cost in execution time. The improved statistical properties are due to the control of polygenic background by two steps. The first step is similar to CIM except for the use of PMLE for the selection of cofactors for markers or interactions between markers, which accounts for the genetic variance due to QTL or QTL epistasis elsewhere in the genome. The additional power of shrinkIM is conferred by the reduction of background toward zero in the case of no QTL at a map position.

More than an extension of PMLE from marker-based mapping to interval mapping, shrinkIM inherits the advantages of shrinkage Bayesian, PMLE and penalized regression. Though a variant of PMLE, PPMLE offers two apparent improvements on PMLE. First, it limits penalization to parameters of interest in order to obtain shrinkage estimation, while exploiting the simplicity of least squares. Second, it eases the dependence of parameter estimates on the prior parameters in PMLE by decreasing the number of penalized parameters in the model.

As a hybrid of shrinkage estimation and least squares, PPMLE is readily extended to handle multi-environment data if the factor effects are treated as fixed. It can also be used for the discovery of genotype-by-environment interaction or for combined analysis based on families from multiple crosses. If collinearity of factors of a genetic model is problematic, we suggest replacing with ridge regression the ordinary least-squares estimate in the first step of PPMLE. As with other regression-based interval mapping methods, parameter estimates are subject to some bias in case of sparse marker maps. This is easily remedied by incorporation of the EM algorithm, in which the probability distribution of QTL genotypes is posterior-updated using the flanking markers and phenotype.

The clean background produced by shrinkIM results from shrinkage estimation of QTL main or epistatic effect. It is reasonable to ask whether QTLs of small effect can be excluded by shrinkage of these effects to zero in the whole-genome scan. Wang *et al.* (2005) showed that the Bayesian shrinkage method could detect a QTL accounting for 2% of phenotypic variance, while Zhang and Xu (2005) showed that PMLE could detect a QTL epistatic effect accounting for only 0.5%. In our simulation shrinkIM detected QTL accounting for 6% phenotypic variance. In practice, the power of shrinkIM may approximate to those of the Bayesian shrinkage method and PMLE because of the similar penalty distribution used in these methods. Further simulation studies should resolve the question.

ShrinkIM combines the merits of the other QTL mapping methods we have considered, in being able to identify QTL or QTL epistasis based on either QTL effect or LOD score. Though shrinkage Bayesian method and PMLE show excellent performance for the detection of QTL or QTL interactions from their effect estimates, the absence of test statistics for the tested QTL remains a problem to apply these methods (Wang *et al.* 2005). In contrast, for conventional interval mapping such as SIM and CIM, LOD is commonly used as evidence to claim a QTL, but the QTL effect profile cannot be used for this purpose because of noisy background. Like the Bayesian approach, shrinkIM supplies QTL evidence by sharpening the QTL effect profile.

The method proposed here may be extended to ECM-based QTL mapping. ShrinkIM is a combination of shrinkage and least squares estimates. Regression-based QTL mapping, though easier to implement and faster to compute, gives biased parameter estimates with sparse markers (Xu 1995) or when QTLs interact or are closely linked (Kao 2001). If we include posterior probability f QTL genotype given flanking markers and observation in step 1 of our algorithm, the method is easily adapted to ECM-based mapping.

ShrinkIM is being incorporated into QGene 4.0, an open-source Java platform for QTL mapping.

References

Boer M. P., Braak C. J. F. and Jansen R. C., 2002 A penalized likelihood method for mapping epistatic quantitative trait loci with one-dimensional genome searches. Genetics **163**: 951-960.

Churchill G. A. and Doerge R. W., 1994 Empirical threshold values for quantitative trait mapping. Genetics **138**: 963-971.

Groß J. 2003. Linear Regression. Springer, Berlin.

Hackett C. A., Meyer R. C. and Thomas W. T. B., 2001 Multi-trait QTL mapping in barley using multivariate regression. Genetic Research **77**: 95-106.

Haley C. S., and Knott S. A., 1992 A simple regression method for mapping quantitative trait loci in line crosses using flanking markers. Heredity **69**:315-324.

Jansen R. C. 1994 Genotype-by-environment interaction in genetic mapping of multiple quantitative trait loci. Theoretical and Applied Genetics **91**: 33-37.

Jiang C., and Zeng Z. B, 1995 Multiple trait analysis of genetic mapping for quantitative trait loci. Genetics **140**: 1111-1127.

Korol A. B., Ronin Y. I., Itskovich A. M., Peng J. and Nevo E., 2001 Enhanced efficiency of quantitative trait loci mapping analysis based on multivariate complexes of quantitative traits. Genetics **157**:1789-1803.

Lander E. S., and Botstein D., 1989 Mapping Mendelian factors underlying quantitative traits using RFLP linkage maps. Genetics **121**:185-199.

Satagopan, J. M., Yandell B. S., Newton M.A. and Osborn T. G., 1996 A Bayesian approach to detect quantitative trait loci using Markov chain Monte Carlo. Genetics **144**: 805–816.

Wang H., Zhang Y. M., Li X., Masinde G. L., Xu S., 2005 Bayesian shrinkage estimation of QTL parameters. Genetics **170**: 465-480.

Xu S., 2003 Estimating polygenic effects using markers of the entire genome. Genetics **163**: 789-801.

Yi N. J., and Xu S., 2000 Bayesian mapping of quantitative trait loci under complicated mating designs. Genetics **157**: 1759-1771.

Zeng Z. B., 1994 Precision mapping of quantitative trait loci. Genetics **136**: 1457-1468.

Zhang Y. M., and Xu S., 2005 A penalized maximum likelihood method for estimating epistatic effect of QTL. Heredity **95**: 96-104.

Figure 2.1 Estimated QTL-effect profiles for single-marker, multiple-marker, and shrinkIM analyses.

a: single-marker; *b*: multiple-marker using PMLE; *c*: multiple-marker Bayesian; *d*: shrinkIM. Asterisks show the true positions and effects of simulated QTL.

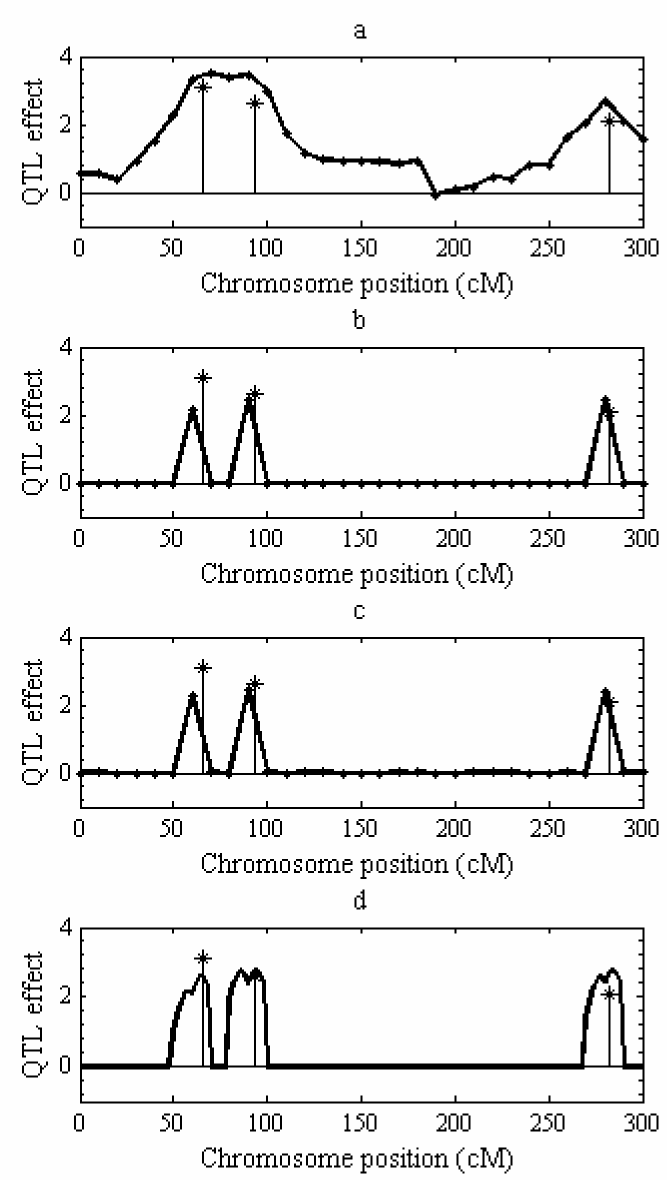

Figure 2.2 Estimated QTL-effect and LOD profiles for SIM, CIM and shrinkIM.

a: SIM; *b*: CIM; *c*: shrinkIM. Asterisks show the true positions of simulated QTL in *a*2, *b*2, *c*2 and their effects in *a*1, *b*1, *c*1. The horizontal dotted lines represent the empirical p = 0.05 LOD thresholds from 1000 permutations.

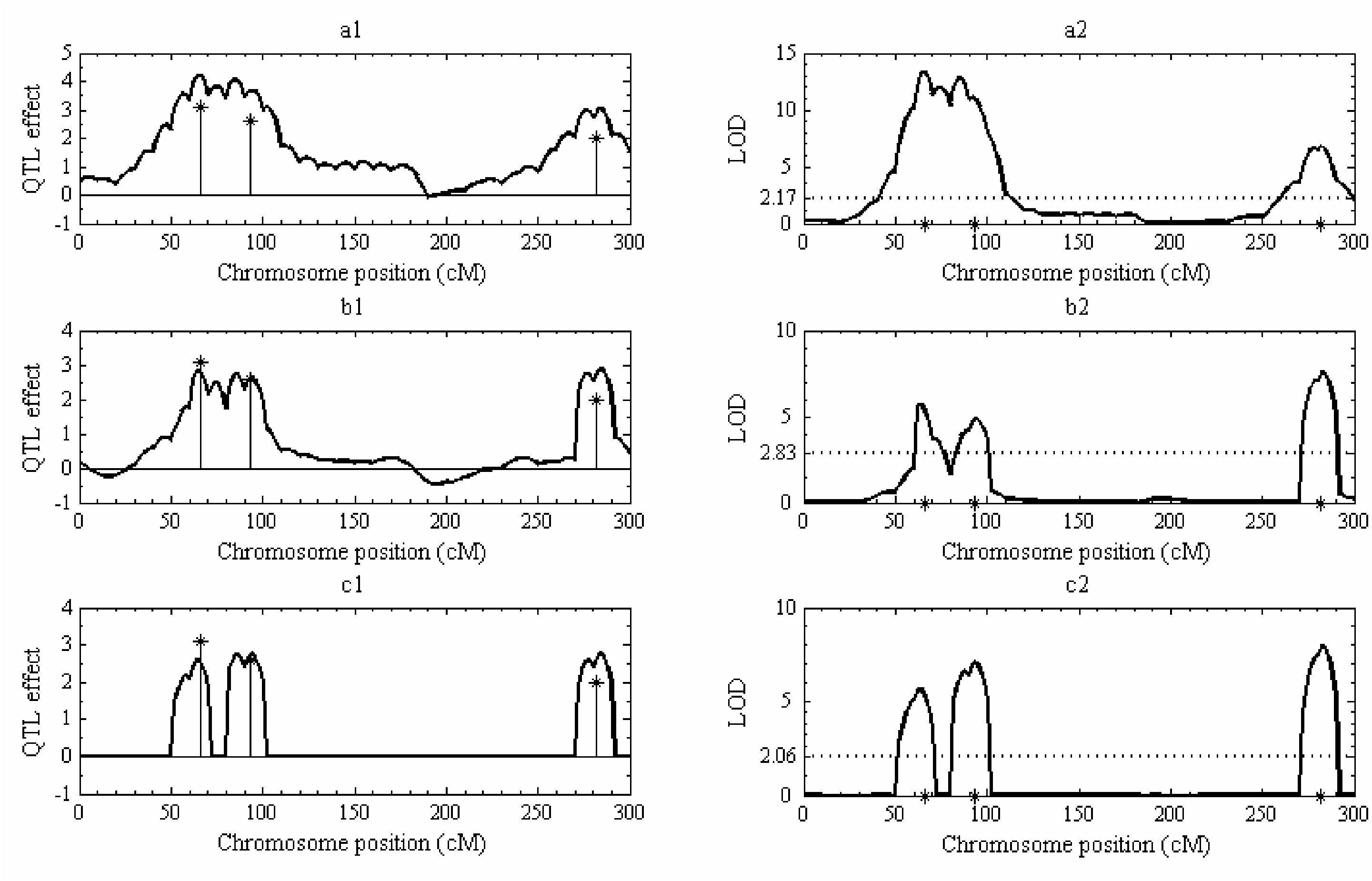

Figure 2.3 3D plots of QTL epistatic effects against chromosome positions for a simulated RIL population.

a: Left of main diagonal: PMLE analysis; right, shrinkIM. *b*: Left, 2D IM; right, shrinkIM.

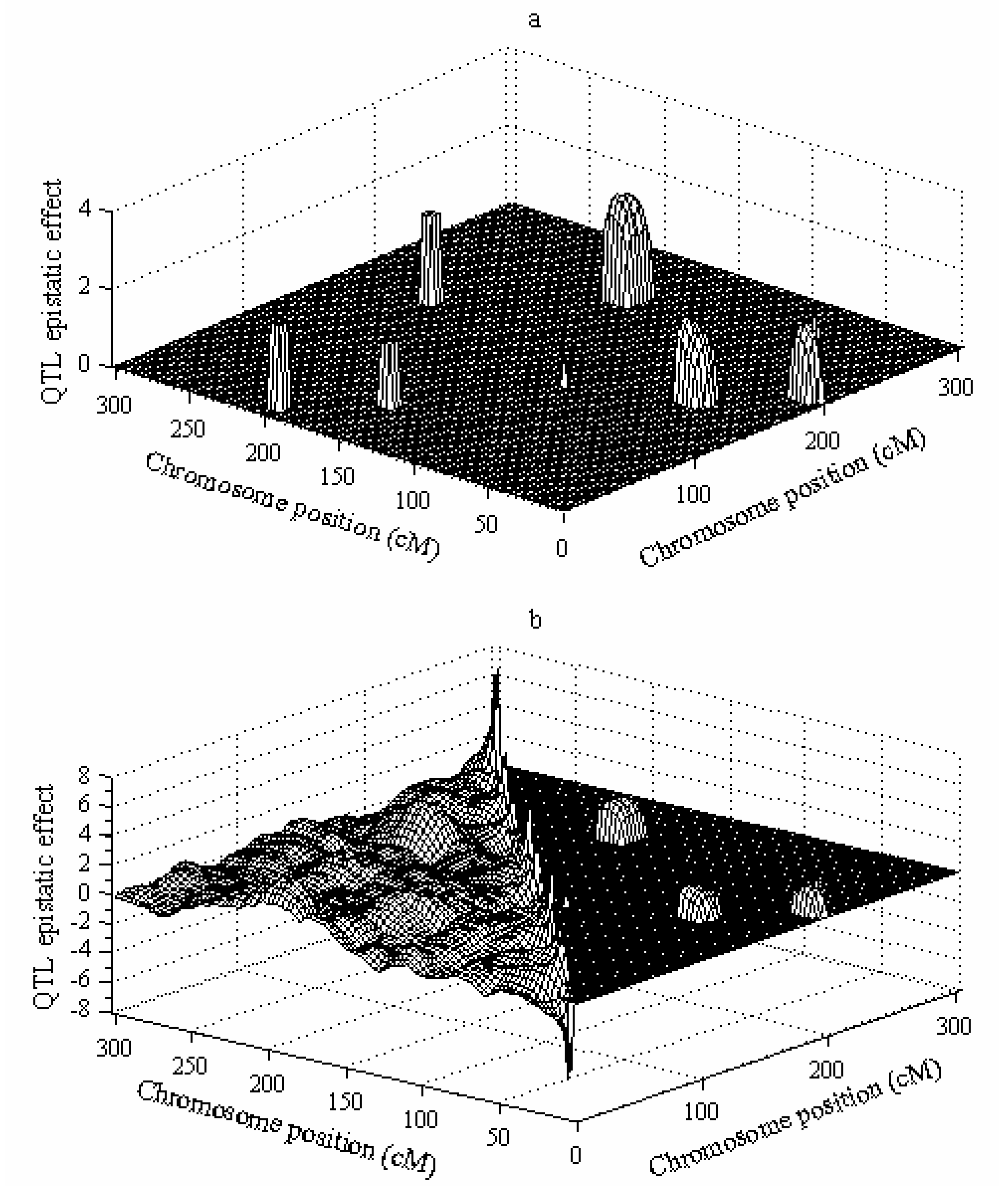

Figure 2.4 3D plots of LOD score of QTL epistasis analysis using 2D IM and shrinkIM. In *a* and *b*, the left-hand side of the figure shows 2D IM and the right-hand side shrinkIM. In *b*, the horizontal surface at LOD 3.39 represents the threshold calculated for 2D IM from 1000 permutations, giving a conservative comparison since the calculated threshold for QTL epistasis analysis using shrinkIM was actually 3.13.

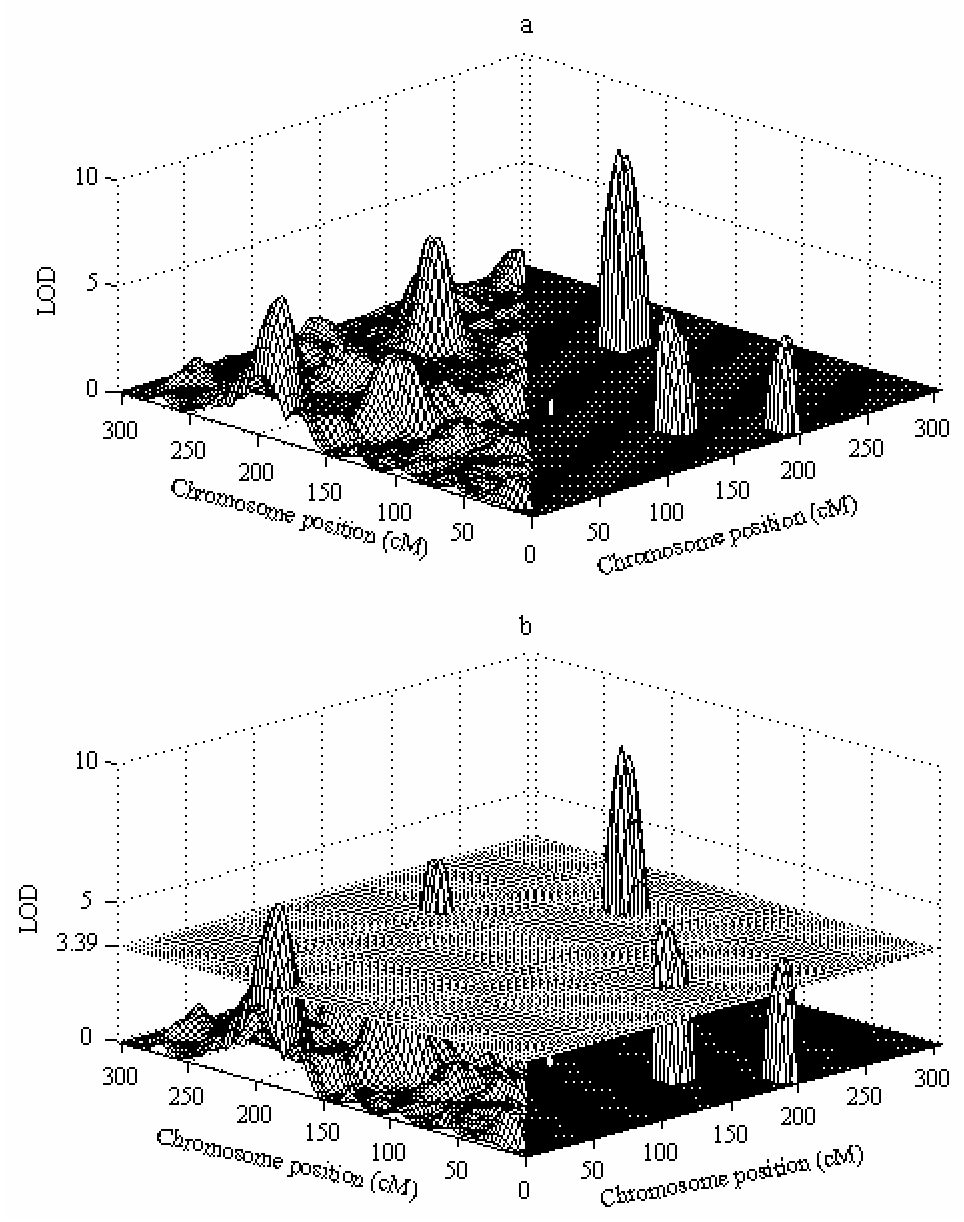

Figure 2.5 The statistical power of QTL detection at three significance levels using SIM, CIM and shrinkIM.

a QTL1; *b* QTL2; *c* QTL3. The white, gray and black bars represent SIM, CIM and shrinkIM.

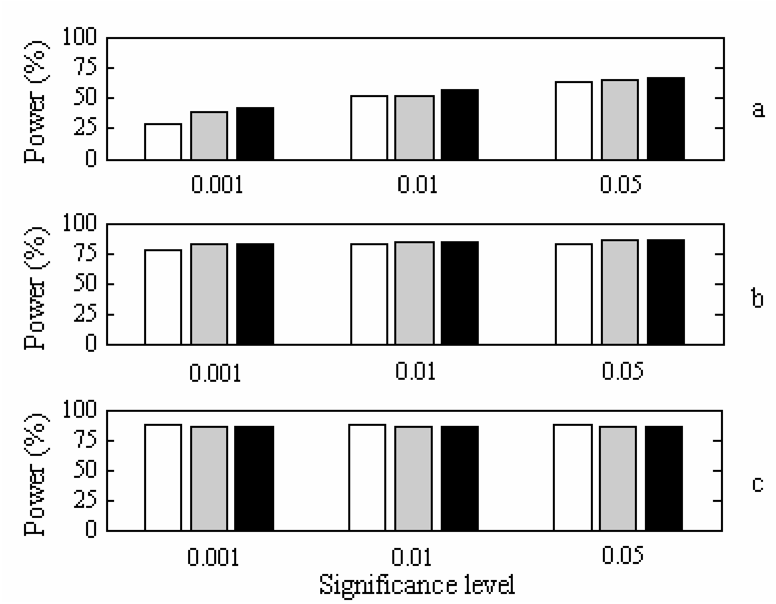

Figure 2.6 LOD profiles produced in the analysis of rice data by SIM, CIM and shrinkIM.

a: SIM; *b*: CIM; *c*: shrinkIM. The horizontal dotted lines in the right-hand plots represent empirical LOD thresholds for the three methods, calculated at significance level 0.05 from 1000 permutation tests. Horizontal axes are on cM scale; labels indicate rice chromosomes.

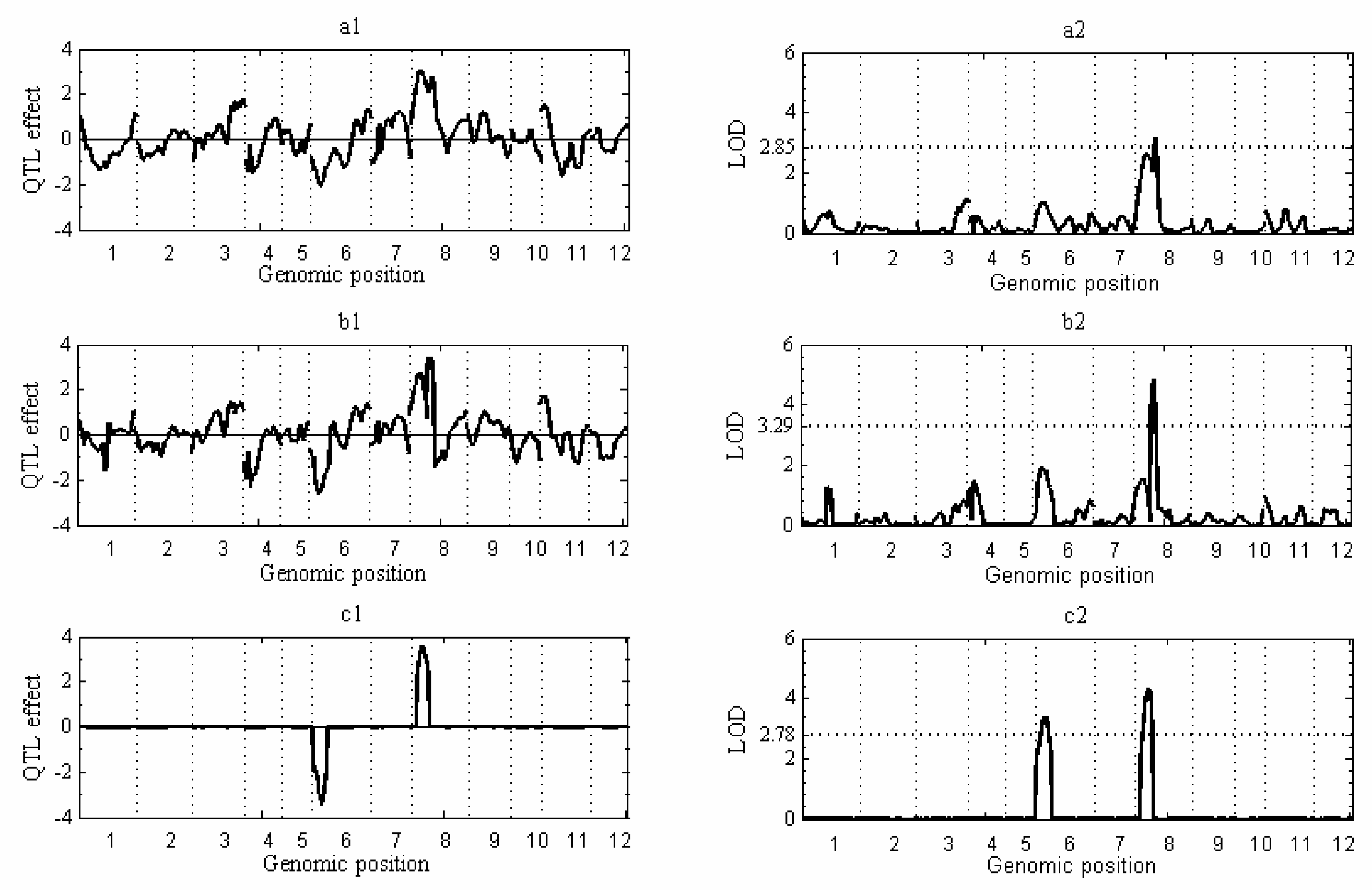

Table 2.1 The true values and estimates of QTL parameters in simulation experiment I. Positions are in cM.

QTL		Main effect		Interaction effect			Environmental variance
		Position	Value	Position 1	Position 2	Value	
1	True values	66	3.1	12	202	2.3	30
2		93	2.6	53	156	1.7	
3		282	2.1	171	237	2.8	
1	Estimates from shrinkIM	66	2.6	12	204	2.1	–
2		94	2.8	54	158	1.6	
3		284	2.8	172	236	2.8	
1	Estimates from PMLE	60	2.1	10	200	2.2	–
2		90	2.4	50	160	1.6	
3		280	2.4	170	240	2.3	

Table 2.2 Computing time required for SIM, CIM and shrinkIM in simulation experiment I

Computing time was evaluated from 1000 permutations for SIM, CIM and shrinkIM. The computer used has a 2-GHz CPU; times are expected to scale similarly on a faster machine

Method	Computing time (sec)
SIM	**32**
EM-SIM	**697**
CIM	**855**
shrinkIM	**348**

Table 2.3 QTL parameters used for simulation experiment II.

Positions are in cM.

QTL	Position	Additive effect	Genetic variance	Proportion	Total variance
1	56	1.7	2.89	0.06	
2	153	2.4	5.76	0.11	
3	282	3.1	9.61	0.18	
Total			18.26	0.35	52.17

Table 2.4 Estimates of QTL positions and effects for rice data using shrinkIM.

Positions are in cM.

QTL	Chromosome	Position	QTL effect	R^2
1	8	36	3.57	0.13
2	6	26	-3.34	0.11

Table 2.5 Comparison of SIM, CIM and shrinkIM in simulation experiment II.

Positions are in cM.

Significance Level	Method	LOD threshold	QTL 1					QTL 2					QTL 3				
			Power (%)	Position	SD	Effect	SD	Power (%)	Position	SD	Effect	SD	Power (%)	Position	SD	Effect	SD
0.05	SIM	2.1	63.2	56.0	2.4	1.96	0.39	82.0	153.3	2.00	2.55	0.41	87.2	282.3	1.71	3.15	0.40
	CIM	2.7	64.6	55.9	2.5	1.86	0.32	85.6	153.3	1.92	2.45	0.37	85.8	282.2	1.62	3.10	0.38
	shrinkIM	2.0	65.8	55.8	2.6	1.62	0.34	86.0	153.3	1.96	2.27	0.43	85.4	282.2	1.55	2.94	0.40
0.01	SIM	2.9	51.6	55.9	2.4	2.07	0.35	82.0	153.2	2.00	2.56	0.41	87.2	282.3	1.71	3.15	0.40
	CIM	3.7	52.2	56.0	2.4	1.95	0.29	85.0	153.3	1.92	2.45	0.37	85.8	282.2	1.62	3.10	0.38
	shrinkIM	2.9	56.0	55.9	2.6	1.71	0.30	84.8	153.3	1.87	2.30	0.39	85.2	282.2	1.65	2.94	0.40
0.001	SIM	4.3	28.6	56.0	2.1	2.30	0.29	78.2	153.2	1.99	2.59	0.38	87.0	282.2	1.70	3.15	0.39
	CIM	4.6	37.8	55.8	2.3	2.06	0.21	83.2	153.3	1.91	2.47	0.36	85.8	282.2	1.55	3.10	0.38
	shrinkIM	4.1	41.8	55.9	2.4	1.84	0.25	82.9	153.3	1.87	2.30	0.39	85.2	282.2	1.64	2.95	0.38

CHAPTER 3 - Multiple-trait quantitative trait locus mapping with incomplete phenotypic data

Abstract

Conventional multiple-trait quantitative trait locus (QTL) mapping methods must discard cases (individuals) with incomplete phenotypic data, thereby sacrificing other phenotypic and genotypic information contained in the discarded cases. Under standard assumptions about the missing-data mechanism, it is possible to exploit these cases. We present an EM-based algorithm that supports conventional hypothesis tests for QTL main effect, pleiotropy, and QTL-by-environment interaction. Simulations confirm improved QTL detection power and precision of QTL location and effect estimation in comparison with case deletion or imputation methods. The EM method may be incorporated into any least-squares or likelihood-maximization QTL-mapping approach.

Introduction

Statistical methods for identifying and mapping genes controlling complex traits, commonly known as quantitative trait loci or QTL, have been developed to a high degree. The primary focus has been on methods for single traits (Lander and Botstein1989; Haley and Knott 1992; Jansen 1993; Zeng 1994; Satagopan *et al.* 1996; Kao and Zeng 1999; Yi and Xu 2003; Wang *et al.* 2005; and many others). It was proposed (Jiang and Zeng 1995; Korol *et al.* 1995) that QTL mapping methods that consider simultaneously several correlated phenotypic traits, or a single trait measured in several environments, offer increased detection power and precision of location and effect estimation over single-trait QTL mapping. This is because trait-by-trait QTL-searching neglects information contained in the data about the common influence of a QTL on more than one trait or in more than one environment. With the promise of increased power from a multivariate approach comes an interesting problem: what to do when some of the multivariate data are missing.

Two main statistical approaches have been elaborated for multi-trait QTL analysis: regression (Korol *et al.* 1995, 1998; Calinski et al. 1999; Knott and Haley 2000; Hackett *et al.* 2001) and maximum likelihood or ML (Jiang and Zeng 1995). Regression QTL-mapping methods, though easier to implement and faster to compute, give biased parameter estimates with sparse markers (Xu 1995) or when QTLs interact or are closely linked (Kao 2001), while ML methods are free of these defects (Kao 2001). It has also been proposed to transform multiple traits into canonical variates so that conventional univariate interval QTL mapping can be applied (Weller *et al.* 1996; Mangin *et al.* 1998; Calinski *et al.* 2000), but interpretation of the results may be difficult.

Though QTL-mapping data are often incomplete, information-recovery methods are at present applied only to genotypic data. For incompletely informative marker-genotype data, posterior distributions are readily estimated from flanking markers in the same individual (Jiang and Zeng 1997). For unknown QTL genotypes at tested positions in map intervals, maximum-likelihood (ML) methods estimate posterior distributions simultaneously with the parameters of a phenotypic mixture distribution (Lander and Botstein 1989), while regression methods (Haley and Knott 1992) replace missing QTL genotypes with their expectations given flanking markers. Variations based on sampling include multiple imputation as described by Sen and Churchill (2001) and Bayesian approaches (*e.g.* Satagopan *et al.* 1996; Sillanpää and Arjas 1998, 1999; Yi and Xu 2001; Wang *et al.* 2005).

In contrast to genotypic data, missing phenotypic data for any trait results in discarding all cases (individuals) lacking even one value, sacrificing all other phenotypic and genotypic information available for these cases. The problem was recognized by Knott and Haley (2000), but they provided no solution. Is there an alternative to this “casewise” (Allison 2002) deletion?

Methods for completion of incomplete multivariate data are of two kinds: by imputation (single or multiple) and by EM algorithm. Single imputation typically replaces missing data with three kinds of values: a value drawn from a specific model-based distribution, a mean calculated from other observations of the same variable, or a conditional mean calculated by least-squares regression on predictors. Multiple imputation (Rubin 1987, 1996) fills in missing data multiple (*e.g.* 3–5) times to produce several complete datasets, with parameter estimates calculated as the average over the results from these datasets. The defect of imputation methods, in analyses such as QTL mapping where we want ML estimates of statistics, is that bias is introduced by maximization of the likelihood over both original and imputed data. In contrast, the EM algorithm as described by Dempster *et al.* (1977) focuses not on replacing a missing value with its expectation, but on using the information available in the original dataset. In the framework of EM, missing data imputed are in effect integrated out of the complete-data log likelihood by iterative refinement of their expectation. Little and Rubin (2001) provided an EM algorithm for incomplete multivariate data, and extended it to accommodate multiple regression with missing responses.

Here we describe an adaptation of Little and Rubin's EM method (2001) to the case of multi-trait QTL mapping with incomplete phenotypic data. We show that the tests for QTL main effects may be constructed as in Jiang and Zeng (1995), and we describe the properties and behavior of the test statistics and QTL effect and position estimates based on simulation studies.

Methods

Missing-data mechanism is ignored: Several kinds of "missingness" have been defined (Rubin 1976). Here we consider only MAR, "missing at random", meaning for our purposes that the probability of missing phenotypic data within any genotype class is unrelated to the phenotypic value. Either for MAR or the stronger assumption, MCAR or "missing completely at random" (missingness also independent of genotype), estimation methods need not model a missing-data mechanism.

Multivariate regression with incomplete data: Consider the linear model

$$\mathbf{Y}_{n\times m} = \mathbf{X}_{n\times p}\mathbf{B}_{p\times m} + \mathbf{E}_{n\times m}, \tag{1}$$

where **Y** is a $(n \times m)$ response matrix with n the number of individuals and m the number of traits (or environments); **X** is a $(n \times p)$ design matrix with p predictors; **E** is an error matrix and $\mathbf{E}_{\mathrm{i}}$ (i = 1, 2, …, n) follows a multivariate normal distribution with means zero and variance–covariance matrix

$$\mathbf{V} = \begin{pmatrix} \sigma_{11}^2 & \sigma_{12}^2 & \cdots & \sigma_{1m}^2 \\ \sigma_{21}^2 & \sigma_{22}^2 & \cdots & \sigma_{2m}^2 \\ \vdots & \vdots & \ddots & \vdots \\ \sigma_{m1}^2 & \sigma_{m2}^2 & \cdots & \sigma_{mm}^2 \end{pmatrix} \tag{2}$$

Suppose there are some missing entries in $\mathbf{Y}_i$ (i = 1, 2, …, n). Now matrices $\mathbf{Y}_i$, $\boldsymbol{\mu}_i = \mathbf{X}_i\mathbf{B}$, and **V** may be partitioned as

$$\mathbf{Y}_i = [\mathbf{y}_i^{obs}, \mathbf{y}_i^{miss}], \tag{3}$$

$$\boldsymbol{\mu}_i = [\boldsymbol{\mu}_i^{obs}, \boldsymbol{\mu}_i^{miss}], \tag{4}$$

$$\mathbf{V} = \begin{bmatrix} \mathbf{V}_{obs(i),obs(i)} & \mathbf{V}_{obs(i),miss(i)} \\ \mathbf{V}_{miss(i),obs(i)} & \mathbf{V}_{miss(i),miss(i)} \end{bmatrix}. \tag{5}$$

For a random sample with n individuals, the log likelihood of observations is given by

$$\ell(\mathbf{B},\mathbf{V};\mathbf{Y}_{obs}) = -\frac{nm}{2}\ln(2\pi) - \frac{1}{2}\sum_{i=1}^{n}\ln\left|\mathbf{V}_{obs,i}\right| - \frac{1}{2}\sum_{i=1}^{n}(\mathbf{y}_i^{obs} - \mathbf{X}_i^{obs}\mathbf{B})^{\mathrm{T}}\mathbf{V}_{obs,i}^{-1}(\mathbf{y}_i^{obs} - \mathbf{X}_i^{obs}\mathbf{B}) \tag{6}$$

Since in general, it is difficult to calculate the MLEs of parameters directly by maximizing (6) with respect to the individual parameters, we may adapt Little and Rubin’s EM (2001) algorithm to obtain the MLEs of parameters in model (1) as follows.

ALGORITHM 1: Starting with initial values $\hat{\boldsymbol{\theta}}^{(0)} = [\hat{\mathbf{B}}^{(0)}, \hat{\boldsymbol{\mu}}^{(0)}, \hat{\mathbf{V}}^{(0)}]$, iterate the following two steps until convergence.

E step:

$$E(\mathbf{y}_i^{miss(k+1)} \left| \mathbf{y}_i^{obs}, \boldsymbol{\theta}^{(k)} \right.) = \hat{\boldsymbol{\mu}}_i^{miss(k+1)} + (\mathbf{y}_i^{obs} - \hat{\boldsymbol{\mu}}_i^{obs(k+1)})\hat{\mathbf{V}}^{(k)}_{\mathbf{y}_i^{obs}\mathbf{y}_i^{miss}}\hat{\mathbf{V}}^{-1(k)}_{\mathbf{y}_i^{obs}\mathbf{y}_i^{obs}}, \tag{7}$$

$$\mathbf{y}_i^{(k+1)} = (\mathbf{y}_i^{obs}, \mathbf{y}_i^{miss(k+1)}). \tag{8}$$

M step:

$$\hat{\mathbf{B}}^{(k+1)} = (\mathbf{X}^{\mathrm{T}}\mathbf{X})^{-1}\mathbf{X}^{\mathrm{T}}\mathbf{Y}^{(k+1)}, \tag{9}$$

$$\hat{\boldsymbol{\mu}}^{(k+1)} = \mathbf{X}\hat{\mathbf{B}}^{(k+1)}, \tag{10}$$

$$\hat{\mathbf{V}}^{(k+1)} = \frac{(\mathbf{Y}^{(k+1)} - \hat{\boldsymbol{\mu}}^{(k+1)})^{\mathrm{T}}(\mathbf{Y}^{(k+1)} - \hat{\boldsymbol{\mu}}^{(k+1)})}{n} \tag{11}$$

Multi-trait QTL mapping with incomplete phenotypic data by regression: We now describe our multi-trait QTL mapping method with incomplete data. Though the method given is based on a recombinant inbred line (RIL) population, it is easily extended to other mating designs such as F_2 or BC. The statistical model for multiple-trait analysis (Jiang and Zeng 1995, Korol *et al.* 1995, Hackett *et al.* 2001) based on complete phenotypic data is

$$\mathbf{Y}_{n\times m} = \mathbf{z}_{n\times 1}\mathbf{a}_{(1\times m)} + \mathbf{x}_{n\times(p+1)}\mathbf{b}_{(p+1)\times m} + \mathbf{E}_{n\times m} \tag{12}$$

where **Y** is a $n \times m$ matrix of phenotypic observations with n lines and m traits and $\mathbf{Y} = [\mathbf{y}_1, \mathbf{y}_2, ..., \mathbf{y}_n]'$, $\mathbf{y}_1, \mathbf{y}_2, \ldots, \mathbf{y}_n$ are $1 \times m$ vectors; **z** is a $n \times 1$ matrix of QTL genotypes represented as 2 for *QQ* and 0 for *qq*; **a** is a $1 \times m$ matrix of additive effects of a putative QTL at a tested position; **x** is a $n \times (p+1)$ matrix of genotypes of p cofactor markers with the first column ones; **b** is a $(p + 1) \times m$ matrix of cofactor marker effects; and **E** is a $n \times m$ matrix of residual errors e_{ij} ($i = 1, 2, \ldots, n$; $j = 1, 2, \ldots, m$), which are assumed to be correlated between traits and follow a multivariate normal distribution with means zero and covariance matrix as in (3). In this model, QTL genotype is replaced with its conditional expectation given flanking-marker genotypes. Least-squares estimates of the parameters can then be obtained by multiple regression.

Now suppose missing values occur in some lines for some traits. Model (12) may be rewritten as model (1)

$$\mathbf{z}_{(n\times 1)}\mathbf{a}_{(1\times m)} + \mathbf{x}_{(n\times(p+1))}\mathbf{b}_{((p+1)\times m)} = \mathbf{X}_{(n\times(p+2))}\mathbf{B}_{((p+2)\times m)}\,. \tag{13}$$

and parameter estimates obtained by ALGORITHM 1.

Multi-trait QTL mapping with incomplete phenotypic data by ECM: Instead of replacing a missing QTL genotype with its expectation given flanking markers, ECM (expectation/conditional maximization) treats QTL genotype as missing data included in model (12) and estimates parameters at a QTL position by repeatedly updating the posterior probability of QTL genotype given both flanking–marker genotypes and phenotypes. Since we now have two types of missing data in model (12), QTL genotype and phenotype, we may extend Jiang and Zeng's (1995) ECM method for multi-trait QTL mapping as follows:

ALGORITHM 2: Starting with initial values of parameters $\boldsymbol{\theta}^{(0)} = [\hat{\mathbf{a}}^{(0)}, \hat{\mathbf{b}}^{(0)}, \hat{\boldsymbol{\mu}}^{(0)}, \hat{\mathbf{V}}^{(0)}]$, iterate the following two steps until convergence.

E step:

$$q_{1i}^{(k+1)} = \frac{p_{1i} f_1^{(k)}(\mathbf{y}_i^{obs} \big| \hat{\boldsymbol{\mu}}_{i,QQ}, \hat{\mathbf{V}}_i)}{p_{1i} f_1^{(k)}(\mathbf{y}_i^{obs} \big| \hat{\boldsymbol{\mu}}_{i,QQ}, \hat{\mathbf{V}}_i) + p_{2i} f_2^{(k)}(\mathbf{y}_i^{obs} \big| \hat{\boldsymbol{\mu}}_{i,qq}, \hat{\mathbf{V}}_i)}, \tag{14}$$

$$q_{2i}^{(k+1)} = \frac{p_{1i} f_2^{(k)}(\mathbf{y}_i^{obs} \big| \hat{\boldsymbol{\mu}}_{i,qq}, \hat{\mathbf{V}}_i)}{p_{1i} f_1^{(k)}(\mathbf{y}_i^{obs} \big| \hat{\boldsymbol{\mu}}_{i,QQ}, \hat{\mathbf{V}}_i) + p_{2i} f_2^{(k)}(\mathbf{y}_i^{obs} \big| \hat{\boldsymbol{\mu}}_{i,qq}, \hat{\mathbf{V}}_i)}, \tag{15}$$

where p_{1i} and p_{2i} are the conditional probabilities of QTL genotypes QQ and qq given flanking markers, f the multivariate normal probability density function, and q_{1i} and q_{2i} the posterior probability of QTL genotypes given flanking markers and phenotypes (Jiang and Zeng 1995).

$$E(\mathbf{y}_i^{miss(k+1)} \big| \mathbf{y}_i^{obs}, \hat{\boldsymbol{\theta}}^{(k)}) = \hat{\boldsymbol{\mu}}_{i,E}^{miss(k+1)} + (\mathbf{y}_i^{obs} - \hat{\boldsymbol{\mu}}_{i,E}^{obs(k+1)})\hat{\mathbf{V}}_{Y_i^{obs}Y_i^{miss}}^{(k)} \hat{\mathbf{V}}_{Y_i^{obs}Y_i^{obs}}^{-1(k)}\,, \tag{16}$$

$$\mathbf{y}_i^{(k+1)} = (\mathbf{y}_i^{obs}, \mathbf{y}_i^{miss(k+1)})\,. \tag{17}$$

M step:

$$\hat{\mathbf{a}}^{(k+1)} = \frac{0.5\mathbf{q}_2^{(k+1)\mathrm{T}}(\mathbf{Y}^{(k+1)} - \mathbf{x}\hat{\mathbf{b}}^{(k+1)})}{\mathbf{q}_2^{\mathrm{T}(k+1)}\mathbf{l}}, \tag{18}$$

where **l** is a (n × 1) matrix of ones.

$$\hat{\mathbf{b}}^{(k+1)} = (\mathbf{x}^{\mathrm{T}}\mathbf{x})^{-1}\mathbf{x}^{\mathrm{T}}[\mathbf{Y}^{(k+1)} - 2\mathbf{q}_2^{(k+1)}\hat{\mathbf{a}}^{(k+1)}], \tag{19}$$

$$\hat{\boldsymbol{\mu}}_E^{(k+1)} = \mathbf{x}\hat{\mathbf{b}}^{(k+1)} + 2\mathbf{q}_2^{(k+1)}\hat{\mathbf{a}}^{(k+1)}, \tag{20}$$

$$\hat{\boldsymbol{\mu}}_{QQ}^{(k+1)} = \hat{\boldsymbol{\mu}}_E^{(k+1)}, \tag{21}$$

$$\hat{\boldsymbol{\mu}}_{qq}^{(k+1)} = \mathbf{x}\hat{\mathbf{b}}^{(k+1)}, \tag{22}$$

$$\hat{\mathbf{V}}^{(k+1)} = \frac{(\mathbf{Y}^{(k+1)} - \hat{\boldsymbol{\mu}}_E^{(k+1)})^{\mathrm{T}}(\mathbf{Y}^{(k+1)} - \hat{\boldsymbol{\mu}}_E^{(k+1)})}{n}. \tag{23}$$

Hypothesis tests: Hypothesis tests for QTL main effects, pleiotropy effects and close linkage vs. pleiotropy are constructed according to Jiang and Zeng (1995) and can be tested by ALGORITHM 1 if regression is chosen or ALGORITHM 2 if the ECM method is used. The test statistic LR or LOD follows an asymptotic chi-square distribution with degrees of freedom determined by the specific hypothesis test (Jiang and Zeng 1995). For example, to test main QTL effects in a two-trait example, the hypotheses can be formulated as H0: $a1 = 0$, $a2 = 0$ and H1: $a1 \neq 0$, $a2 \neq 0$. For the regression method, parameters under H0 or H1 are estimated by ALGORITHM 1 (Equations 7–11) depending on whether or not QTL effects are included in model (13). If the ECM method is used, first these quantities are estimated under H0 by ALGORITHM 1 without inclusion of QTL effect and then those of the full model under H1 can be obtained by ALGORITHM 2 (Equations 14–23). Then the likelihood ratio (LR) can be obtained as $LR = -2(\ell_{reduced} - \ell_{full})$, where $\ell_{reduced}$ is the log likelihood of the reduced model, corresponding to H0, and ℓ_{full} is that of the full model, corresponding to H1 (Lander and Botstein 1989). Both are calculated from (6) and a LOD score is calculated as LR/(2 ln 10).

Simulation methods: To compare the properties of the EM method with those of casewise deletion (CaD), mean substitution (MS), conditional mean substitution (CMS) and complete data (CoD), we performed simulation experiments. RIL populations from line crosses with 100, 200 and 300 individuals were generated based on a 300-cM chromosome with 31 evenly spaced markers. For CMS, missing data were replaced with their conditional expectations calculated by regression of each trait on the other(s). Three pleiotropic QTLs controlling two traits were simulated at cM positions 53, 182, and 258 with effects listed in Table 3.1. Trait values of each line were calculated as the sum of QTL effects plus a random vector of environmental effects with means zero and variance given in Table 1. Then a specified proportion (0.05, 0.10, 0.20, or 0.40) of values for each trait independently were set to missing. Lines lacking data for both traits were dropped. Analyses were performed on 500 replicates.

In the QTL analyses, the calculation interval (step size) used was 1 cM. Cofactor markers for each trait were selected by forward stepwise regression at a significance level of 0.01 and combined for multi-trait analysis. Cofactors lying within 10 cM of a QTL testing position were dropped from the model. Genome-wide LOD thresholds of 3.71, 3.54 and 3.43 for n = 100, 200, and 300 at significance level 0.05 were calculated from 5000 simulations under the null hypothesis of no QTL (Knott and Haley 2000). When sample size or heritability is relatively small, the effect of a QTL may extend to adjacent intervals due to limited recombination between these intervals and the QTL. So a QTL was declared if a LOD peak higher than threshold was found within the interval containing the simulated QTL and its two flanking intervals. Power of QTL detection was calculated as the number of correctly declared (“true positive”) QTLs divided by the number of actual QTLs simulated, while specificity was calculated as the number of true positive QTLs divided by the number of QTLs declared.

Results

Power: As expected, power was highest when data were complete (Table 3.2, Figure 3.1). When data were missing, EM, MS and CMS gave power superior to CaD in all cases. MS and CMS gave similar power, equal to or lower than that of EM. The gain in power for EM over CaD increased with the proportion of missing data. This trend was also seen for gain in power of EM over MS or CMS, but to a lower degree.

In Table 3.2, it is seen that EM gave QTL detection power about equal to that supplied by CaD with half the proportion of missing data. Simple probability calculations yield the numbers to which this power relationship corresponds. As an example, in a population of size 300 with 0.4 of the data missing from each of two traits, the EM method was operating on only 108 lines carrying complete data and another 144 lines with partial data, but achieved power corresponding to approximately 192 lines with complete data. The increase in effective (equivalent-power) number of complete records achieved by the EM method can be estimated graphically from Figure 3.2. Here the effective complete-data sample sizes achieved by EM were about 271, 255, 230, and 190, representing gains of 1, 12, 38 and 82 over the number of complete records available for CaD at missing levels of 0.05, 0.1, 0.2 and 0.4.

Specificity and QTL position: All the methods gave similar specificity for QTL detection, except that CaD gave decreased specificity with increasing proportions of missing data (Table 3.3).

Accuracy and precision of effect estimation: All methods gave reasonable estimates of QTL positions. CoD and CaD provided the highest and lowest precisions for QTL position estimation (Figure 3.3), while those of MS, MS, and EM were very similar and intermediate. For QTL effects (Figure 3.4), CoD, CaD and EM provided unbiased estimates, while both MS and CMS underestimated these parameters, CMS by slightly less. The extent of underestimation tended to increase with missing percentage and decrease with sample size (not shown here).

Discussion

The EM-based multi-trait QTL mapping method we propose here is superior to mean substitution and conditional mean substitution for several reasons. MS underestimates phenotypic variation and QTL effect due to fill-in of missing data with a single value, resulting in decreased power compared with our method especially when amounts of missing data are relatively large. The same trend can be observed for CMS, which, as a precursor of the EM algorithm, is closely related to a single EM iteration (Little and Rubin 2001). Although CMS improved estimates of QTL effect compared with MS, it still underestimates variance (Little and Rubin 2001).

While we did not include multiple imputation (Rubin 1987, 1996) (MI) in the simulation study, we doubt its potential utility for multi-trait QTL mapping with missing trait data. We investigated MI by filling in missing trait data with values sampled from their conditional distribution under the null and alternative hypotheses given the observed trait values. Resulting LOD profiles were sawtoothed (Fig.3.5) due to random sampling, and a different profile could be obtained with each analysis even with many imputations (*e.g.* 100 compared with 3–5 in regular MI) performed at each QTL test position. For these reasons, apart from the high computational cost, we did not pursue this method further.

For MS, CMS, and even MI, the effects of introducing imputed data on QTL mapping need further study. Although simulation results showed specificities close to those of our method, complete-data analysis, and casewise deletion, the bias imposed on the LOD test statistic by introduction of these “artificial” data remains unknown. In fact, imputation of missing data is also performed in the E step of our EM algorithm. But this kind of imputation only furnishes a pivot to facilitate parameter estimation and is actually not involved in the likelihood calculation. Thus, theoretically, the EM-based method does not bias QTL detection and parameter estimation as may imputation methods.

The information gain of our method over CaD, MS, and CMS depends on the amount of missing trait data. The reason is readily explained by the following example for CaD. Consider a sample of 200 individuals with missing proportion 0.1 for each of two traits independently. The average number of individuals available for CaD is 162 and that for EM 198, and the difference is 36. This difference expands to 96 with a missing proportion of 0.4. In other words, power is lost more slowly with data loss when the information-recovering EM method is applied.

Some extensions of the EM method are promising. First, we have derived the EM calculation of the hypothesis test for QTL main effect. By following the procedure of Jiang and Zeng (1995), one may derive specific EM implementations for other hypothesis tests including for QTL-by-environment interaction, pleiotropy, and pleiotropy vs. close linkage. Second, the EM method may be extended to multiple interval mapping (Kao *et al.* 1999) with multiple traits and incomplete phenotypic data. Third, mixed-model QTL mapping as recommended by Jiang and Zeng (1995) can now be applied to incomplete trait data as an alternative method for multi-trait QTL mapping. When multiple traits are actually different expressions of a single trait in different environments (locations or years), a mixed model allows treating environmental effect as a random and QTL effect as a fixed factor (Wang *et al.* 1999; Piepho 2000). One of the advantages of the mixed model is in accommodating both balanced and unbalanced data structure.

The method we have presented requires more computing time than the conventional EM or ECM interval-mapping algorithm. There are two reasons for this. First, to obtain parameter estimates, the EM algorithm must be applied under both null and alternative hypotheses, because the trait data are missing in both cases. In contrast, conventional methods require EM iteration only under the alternative hypothesis. Second, our EM algorithm is used to complete both QTL genotype and phenotype in the case of ML-based QTL mapping, while the conventional method must complete only QTL genotype. The computing load increases with the proportion of missing data, but the extreme amounts of missing data we have simulated are unusual in real experiments.

References

Allison P. D., 2002 Missing Data. Sage Publications, Thousand Oaks, Calif.

Calinski T., Kaczmarek Z., Krajewski P., Frova C. and Sari-Gorla M., 1999 A multivariate approach to the problem of QTL localization. Heredity **84**: 303-310.

Churchill G. A., and Doerge R. W., 1994 Empirical threshold values for quantitative trait mapping. Genetics **138**: 963-971.

Dempster A. P., Laird N. M. and Rubin D. B., 1977 Maximum likelihood from incomplete data via the EM algorithm. Journal of the Royal Statistical Society **39**: 1-38.

Hackett C. A., Meyer R. C. and Thomas W. T. B., 2001 Multi-trait QTL mapping in barley using multivariate regression. Genetical research **77**: 95-106.

Haley C. S. and Knott S. A., 1992 A simple regression method for mapping quantitative trait loci in line crosses using flanking markers. Heredity **69**: 315-324.

Jansen R. C., 1993 Interval mapping of multiple quantitative trait loci. Genetics 135: 205-211.

Jiang C. J. and Zeng Z. B., 1995 Multiple trait analysis of genetic mapping for quantitative trait loci. Genetics **140**: 1111-1127.

Jiang C. J. and Zeng Z. B., 1997 Mapping quantitative trait loci with dominant and missing markers in various crosses from two inbred lines. Genetics **101**: 47-58

Kao C. H., 2000 On the difference between maximum likelihood and regression interval mapping in the analysis of quantitative trait loci. Genetics **156**: 855-865.

Kao C. H., Zeng Z. B. and Teasdale R. D., 1999 Multiple interval mapping for quantitative trait loci. Genetics **152**: 1203-1216.

Knott S. A. and Haley C. S., 2000 Multitrait least squares for quantitative trait loci detection. Genetics **156**: 899-911.

Korol A. B., Ronin Y. I. and Kirzhner V. M.. 1995 Interval mapping of quantitative trait loci employing correlated trait complexes. Genetics **140**: 1137-1147.

Korol A. B., Ronin Y. I., Nevo E. and Hayes P. M.. 1998 Multi-interval mapping of correlated trait complexes. Heredity **80**: 273-284.

Lander E. S., and Botstein D., 1989 Mapping Mendelian factors underlying quantitative traits using RFLP linkage maps. Genetics **121**: 185-199.

Little R. J. A. and Rubin D. B., 2001 Statistical Analysis with Missing Data. John Wiley & Sons, Hoboken, New Jersey.

Mangin B., Thoquet P. and Grimsley N., 1998 Pleiotropic QTL analysis. Biometrics **54**: 88-99.

Sillanpää M. J. and Arjas E., 1998 Bayesian mapping of multiple quantitative trait loci from incomplete inbred line cross data. Genetics **148**: 1373-1388.

Sillanpää M. J. and Arjas E., 1999 Bayesian mapping of multiple quantitative trait loci from incomplete outbred offspring data. Genetics **151**: 1605-1619.

Piepho H. P., 2000 A mixed-model approach to mapping quantitative trait loci in barley on the basis of multiple environment data. Genetics **156**: 2043-2050 .

Rubin D. B., 1976 Inference and missing data. Biometrika **63**: 581-592.

Rubin D. B., 1987 Multiple Imputation for Nonresponse in Surveys. Wiley, New York.

Rubin D. B., 1996 Multiple imputation after 18+ years. Journal of the American Statistical Association **91**: 473-489.

Satagopan J. M., Yandell B. S., Newton M. A. and Osborn T. G., 1996 A Bayesian approach to detect quantitative trait loci using Markov chain Monte Carlo. Genetics **144**: 805–816.

Sen S. and Churchill G. A., 2001 A statistical framework for quantitative trait mapping. Genetics **159**: 371–387.

Wang D. L., Zhu J., Li Z. K. and Paterson A. H., 1999 Mapping QTLs with epistatic effects and QTL×environment interactions by mixed linear model approaches, Theoretical and Applied Genetics **99**: 1255-1264

Wang H., Zhang Y. M., Li X., Masinde G. L., Mohan S., 2005 Bayesian shrinkage estimation of QTL parameters. Genetics **170**: 465-480.

Weller J. I., Wiggans G. R., Van Raden P. M. and Ron M., 1996 Application of a canonical transformation to detection of quantitative trait loci with the aid of genetic markers in a multi-trait experiment. Theoretical and Applied Genetics **92**: 998-1002.

Yi N. J., and Xu S., 2001 Bayesian mapping of quantitative trait loci under complicated mating designs. Genetics **157**: 1759-1771.

Figure 3.1 Statistical power of five multiple-trait QTL-mapping methods with four levels of missing data.

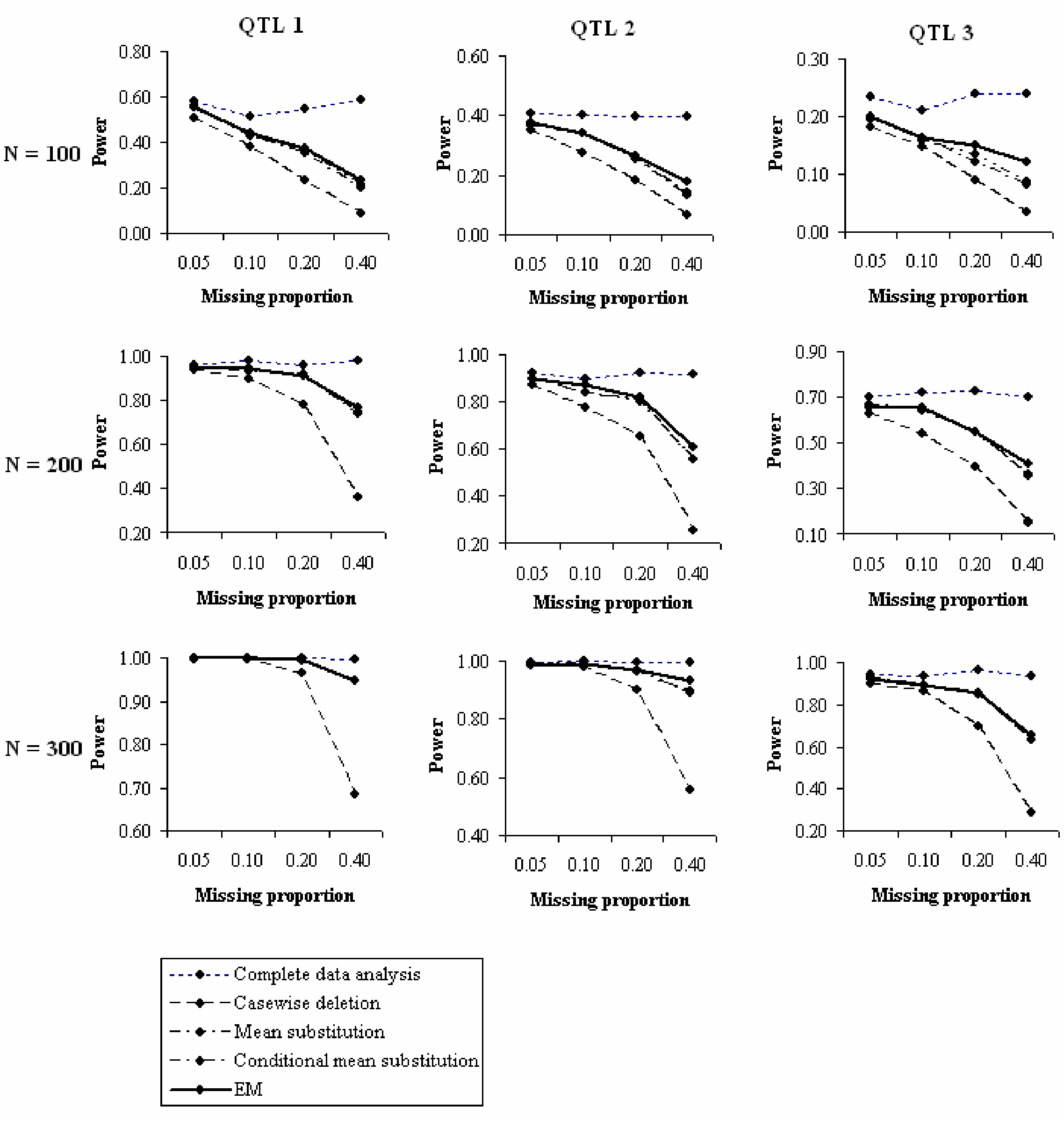

Figure 3.2 Power of QTL 1 detection after casewise deletion and by the EM method as a function of the number of complete trait records.

The power used is evaluated over 500 replicates of simulations with 200 RILs.

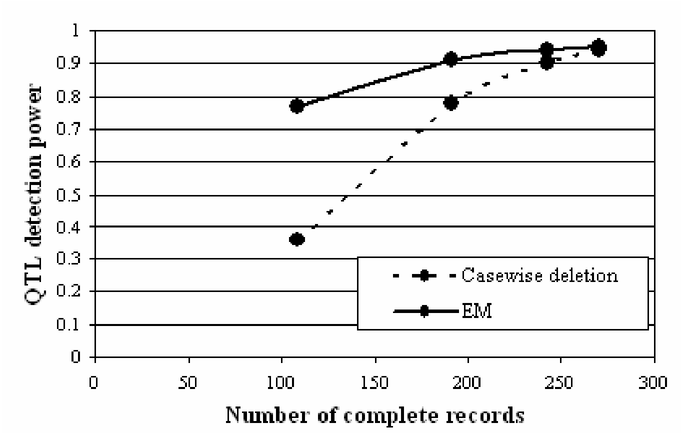

Figure 3.3 Means and standard deviations (SDs) of estimates of QTL position by multi-trait QTL analyses.

Means and SDs of estimates of QTL position were calculated over 500 replicates of simulations with 200 RILs. Missing percentage for each trait is 0.40. White, gray and black bars represent QTLs 1, 2 and 3. CoD: complete data analysis; CaD: casewise deletion; MS: mean substitution; CMS: conditional mean substitution; EM: EM algorithm.

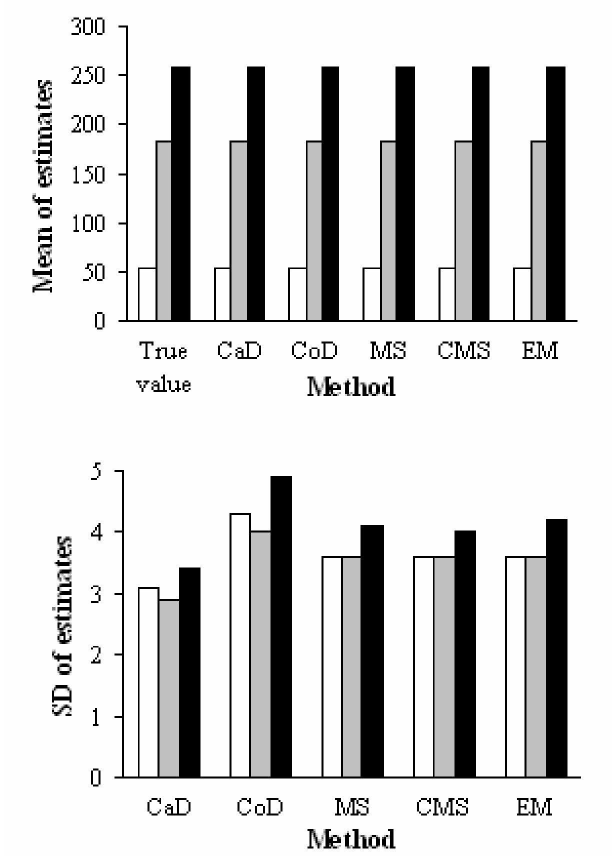

Figure 3.4 Means and standard deviations (SDs) of estimates of QTL effects by multi-trait QTL analyses.

Means and SDs of estimates of QTL position were calculated over 500 replicates of simulations with 200 RILs. Missing percentage for each trait is 0.40. White and gray bars represent trait 1 and 2. CoD: complete data analysis; CaD: casewise deletion; MS: mean substitution; CMS: conditional mean substitution; EM: EM algorithm.

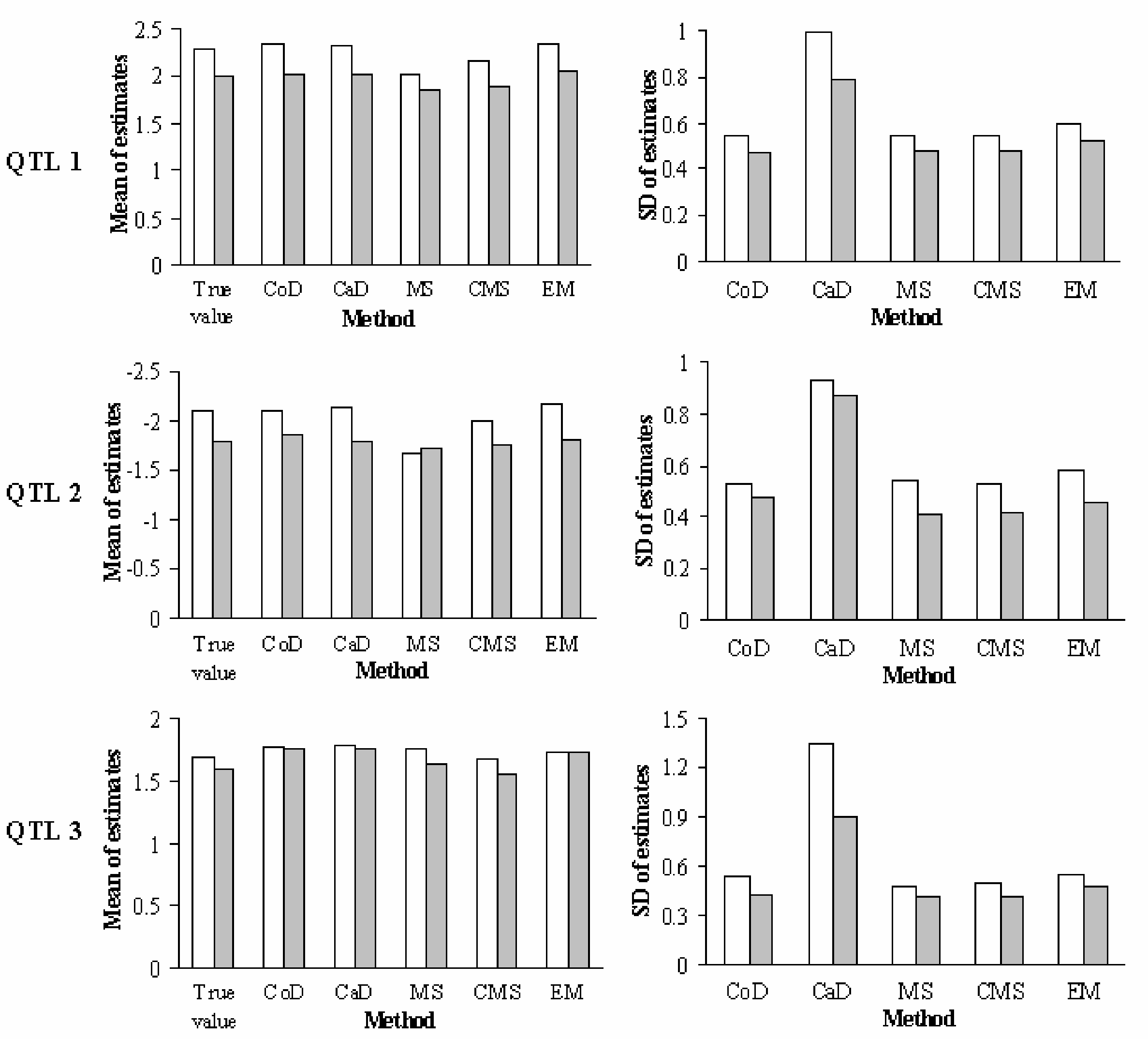

Figure 3.5 LOD profile produced by multiple-imputation method for multi-trait QTL analysis based on simulated data.

The sample analyzed was simulated with 200 individuals and 0.2 missing proportion. The missing trait values were imputed 50 times at each QTL test position and the LOD score in the plot was calculated as an average of the LODs obtained from multi-trait QTL analysis of each imputed data set. Asterisks show the true positions of simulated QTLs.

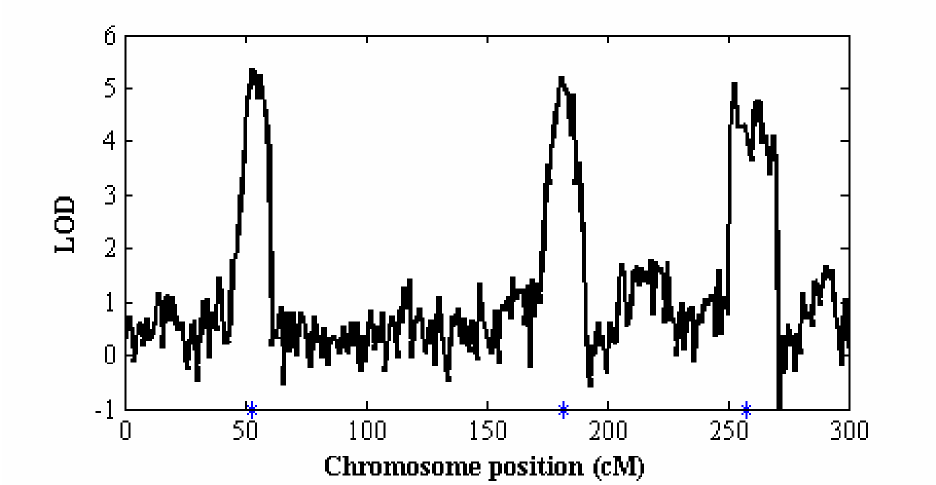

Table 3.1 QTL effects and variances for two traits used for simulation of multi-trait QTL mapping.

Parameter	**QTL**	**Trait**	
		1	**2**
QTL effect	1	2.3	2
	2	-2.1	-1.8
	3	1.7	1.6
QTL variance	1	5.29 (8.40%)	4.00 (8.16%)
	2	4.41 (7.01%)	3.24 (6.61%)
	3	2.89 (4.59%)	2.56 (5.22%)
Total genetic variance		12.6 (20%)	9.80 (20%)
Environmental variance		50.0 (80%)	39.2 (80%)
Phenotypic variance		62.6 (100%)	49.0 (100%)

Table 3.2 Observed statistical power of five multi-trait QTL mapping methods

Sample	Missing	QTL 1					QTL 2					QTL 3				
size	proportion	CoD	CaD	MS	CMS	EM	CoD	CaD	MS	CMS	EM	CoD	CaD	MS	CMS	EM
100	0.05	0.58	0.51	0.55	0.56	0.55	0.41	0.35	0.36	0.37	0.38	0.23	0.18	0.20	0.20	0.20
	0.10	0.51	0.38	0.43	0.42	0.44	0.40	0.28	0.34	0.34	0.34	0.21	0.15	0.16	0.16	0.16
	0.20	0.55	0.24	0.36	0.37	0.37	0.40	0.18	0.26	0.25	0.26	0.24	0.09	0.12	0.13	0.15
	0.40	0.59	0.09	0.20	0.21	0.24	0.40	0.07	0.13	0.14	0.18	0.24	0.03	0.08	0.09	0.12
200	0.05	0.96	0.94	0.95	0.95	0.95	0.92	0.87	0.90	0.90	0.90	0.70	0.62	0.66	0.66	0.66
	0.10	0.98	0.90	0.93	0.93	0.94	0.90	0.77	0.84	0.84	0.87	0.72	0.54	0.64	0.65	0.65
	0.20	0.96	0.78	0.91	0.91	0.91	0.92	0.65	0.81	0.80	0.82	0.73	0.39	0.54	0.54	0.55
	0.40	0.98	0.36	0.75	0.74	0.77	0.91	0.26	0.55	0.56	0.61	0.70	0.16	0.35	0.36	0.41
300	0.05	1.00	1.00	1.00	1.00	1.00	1.00	0.98	0.99	0.99	0.99	0.94	0.90	0.93	0.93	0.92
	0.10	1.00	1.00	1.00	1.00	1.00	1.00	0.98	0.98	0.99	0.99	0.94	0.86	0.89	0.89	0.89
	0.20	1.00	0.96	0.99	0.99	1.00	1.00	0.90	0.96	0.97	0.97	0.96	0.69	0.85	0.85	0.85
	0.40	1.00	0.68	0.95	0.95	0.95	1.00	0.56	0.89	0.89	0.93	0.94	0.28	0.63	0.63	0.66

Table 3.3 Observed statistical specificity of multi-trait QTL analyses

Sample	Missing	Mapping method				
size	proportion	CoD	CaD	MS	CMS	EM
100	0.05	0.99	0.98	0.98	0.98	0.98
	0.10	0.99	0.98	0.99	0.99	0.99
	0.20	0.99	0.97	0.98	0.98	0.98
	0.40	0.99	0.93	0.98	0.99	0.98
200	0.05	0.99	0.99	0.99	0.99	0.99
	0.10	1.00	0.99	1.00	1.00	0.99
	0.20	0.99	0.99	0.99	0.99	1.00
	0.40	1.00	0.97	0.99	0.99	0.99
300	0.05	0.99	0.99	0.99	0.99	0.99
	0.10	0.99	0.99	0.99	0.99	0.99
	0.20	0.99	0.98	0.99	0.99	0.99
	0.40	0.99	0.98	0.99	0.99	0.99